

# **Nanotechnology for smart applications: Vol. 1-Nanotechnology for biomedical applications**

## **Carbon nanotubes for biomedical applications**

Mafalda R. Almeida<sup>1</sup>, João C. F. Nunes<sup>1</sup>, Raquel O. Cristóvão<sup>2</sup>, Joaquim L. Faria<sup>2</sup>, Ana P. M.

Tavares<sup>1\*</sup>, Cláudia G. Silva<sup>2</sup>, Mara G. Freire<sup>1</sup>

<sup>1</sup>CICECO-Aveiro Institute of Materials, Department of Chemistry, University of Aveiro, 3810-193 Aveiro, Portugal

<sup>2</sup>Laboratory of Separation and Reaction Engineering - Laboratory of Catalysis and Materials (LSRE-LCM), Department of Chemical Engineering, Faculty of Engineering, University of Porto, 4200-465 Porto, Portugal

**\*Corresponding author:**

Ana P. M. Tavares:

E-mail: aptavares@ua.pt; Tel: +351 234 401 520

## List of abbreviations

$^1\text{O}_2$  – singlet oxygen  
99mTc – technetium-99m  
AF488/647 – Alexa-fluor  
ALG – alginate  
AT1R – angiotensin II type 1 receptor  
AT2R – angiotensin II type 2 receptor  
AuNPs – gold nanoparticles  
AZ – azoxystrobin  
BA – betulinic acid  
BrdU – bromodeoxyuridine  
BSA – bovine serum albumin  
CDDP – cisplatin  
Ce6 – chlorin e6  
CEA – carcinoembryonic antigen  
CHI – chitosan  
CHI-F – chitosan-folate  
CNTs – carbon nanotubes  
CNx-MWCNTs – nitrogen-doped multi-walled carbon nanotubes  
CP – carboplatin  
CPT – camptothecin  
DDS – drug delivery systems  
dendrimerFc – ferrocene-grafted dendrimer  
DEX – dexamethasone  
dMWCNTs – polyamidoamine dendrimer modified multi-walled carbon nanotubes  
DNA – deoxyribonucleic acid  
Docel™ – commercial DTX injection  
DOX – doxorubicin  
DRG – dorsal root ganglion  
DTX – docetaxel  
DWCNTs – double-walled carbon nanotubes  
EAC – Erlich ascites carcinoma  
EpCAM – epithelial cell adhesion molecule  
FA – folic acid  
FA-PEG – folic acid-terminated polyethylene glycol  
fCNTs – functionalized carbon nanotubes  
FI – fluorescein isothiocyanate  
fMWCNTs – functionalized multi-walled carbon nanotubes  
FR – folate receptor  
Gd – gadolinium  
GO – graphene oxide  
GOx – glucose oxidase  
GR – graphene  
HA – hyaluronic acid  
hapten AZc6 – carboxylated spacer arm  
HER2 – human endothelial receptor 2  
HIF-1 $\alpha$  – hypoxia-inducible factor 1 alpha  
HMME – hematoporphyrin monomethyl ether  
IGF1R – insulin-like growth factor 1 receptor  
IgY – immunoglobulin Y  
iRGD – tumor-homing peptide

Lys – lysine  
MDA-MB-231 – human breast carcinoma cells  
MDM2 – murine double minute clone 2  
MNs – magnetic nanoparticles  
MOF – metal oxide framework  
MSCs – marrow stromal cells  
mTHPC – m-tetrahydroxyphenylchlorin  
MTX – methotrexate  
MWCNTs – multi-walled carbon nanotubes  
Nf – nafion  
NGR – asparagine-glycine-arginine peptide  
Ni – nickel  
pAT2 – plasmid AT2  
PBS – phosphate-buffered saline  
PCA – poly citric acid  
pDNA – plasmid deoxyribonucleic acid  
PDT – photodynamic therapy  
PLK1 – Polo-Like Kinase1  
PL-PEG – phospholipid molecules with polyethylene glycol  
PPy – polypyrrole  
Pt – platinum  
PTT – photothermal therapy  
PTX – paclitaxel  
Pyrr – pyridinium  
RAS – renin-angiotensin system  
RES - reticuloendothelial system  
RGD – cyclic peptide composed of 9 amino acids  
rhBMP-2 – recombinant human bone morphogenetic protein-2  
ROS – reactive oxidative species  
RTA – recombined ricin A chain protein  
SA – streptavidin  
SDS - sodium dodecyl sulfate  
siCas 3 – small-interfering caspase-3  
siRNA – small-interfering ribonucleic acid  
siTOX – cytotoxic small-interfering ribonucleic acid sequence  
SS – cystamine  
ssDNA AP – single-stranded deoxyribonucleic acid aptamer  
SWCNTs – single-walled carbon nanotubes  
TAM – tamoxifen  
Tf – transferrin  
TPGS – D- $\alpha$ -Tocopherol polyethylene glycol 1000 succinate  
TRAIL – tumor necrosis factor-related apoptosis-inducing ligand  
VA – vertically aligned  
VP-16 – etoposide

## **Abstract**

Carbon nanotubes (CNTs) were discovered in 1991, and since then, have been one of the most intensely studied nanomaterials due to their improved functionalities and diversity of applications. Specifically, CNTs are entirely composed of carbon atoms connected through  $sp^2$  bonds structured in several condensed benzene rings rolled up into a cylinder form. Depending on the number of graphitic layers, CNTs can be classified into single-walled carbon nanotubes (SWCNTs) or multi-walled carbon nanotubes (MWCNTs). The specific structural properties of CNTs, leading to a strong loading capacity, high surface area, high strength, and enhanced chemical and thermal stability, make these nanomaterials very promising for biomedical applications. In this sense, this book chapter overviews the potential applications of CNTs in the biomedical field, highlighting their usage on: (1) diagnosis, by the development of CNTs-based biosensors and imaging methods; (2) tissue engineering; (3) delivery systems of several anticancer and antihypertensive drugs, corticosteroids, genes, nucleic acids, among others; and (4) target therapies, namely photothermal and photodynamic therapies. Additionally, particular attention is given to the CNTs potential toxicity and different strategies to overcome this controversial subject, namely by the adequate CNTs functionalization.

## **Keywords**

Carbon nanotubes; biomedical applications; diagnosis; tissue engineering; delivery systems; target therapies.

## 1. Introduction

Due to their peculiar properties and nanoscale dimensions, nanomaterials have been largely used as biomaterials in several fields of applications. Specifically, in biomedicine, these miniaturized particles, whose dimensions are in line with those of the living cells, have been opening new and important applications. Among nanoparticles, and particularly due to their chemical and physical properties, carbon-based nanomaterials are becoming highly attractive for biomedical applications, namely for cancer diagnosis and therapy, cell and tissue engineering, targeted drug delivery, and biosensing [1–3]. According to the structural arrangement of their atoms, there are several carbon allotropes, with fullerenes, carbon nanotubes (CNTs) and graphene oxide (GO) being the most used in the field of biomedicine [4, 5].

CNTs were discovered in 1991 by Sumio Iijima [6] using transmission electron microscopy. Since then, they have been one of the most intensely studied nanomaterials, with thousands of reports on a wide variety of applications [7]. CNTs provide improved functionalities due to their specific structural properties [8], strong loading capacity [9], designed biocompatibility [10], high surface area, high strength, and enhanced chemical and thermal stability [11].

CNTs consist entirely of carbon atoms connected through  $sp^2$  bonds structured in several condensed benzene rings rolled up into a cylinder form, presenting lengths in the order of  $\mu\text{m}$  and diameters up to 100 nm [12]. The orientation of benzene rings along the cylindrical surface dictates their metallic, semiconducting, or superconducting electron transport properties [13, 14]. Depending on the number of graphitic layers, CNTs are classified into single-walled carbon nanotubes (SWCNTs) or multi-walled carbon nanotubes (MWCNTs). SWCNTs own the simplest morphology, consisting of a single layer of graphene with diameters between 0.4 and 2 nm, generally existing as hexagonal close-packed bundles. MWCNTs comprise two or more concentric cylinders, each made of a single graphene sheet surrounding a hollow core with inner diameters between 1 and 3 nm. The outer diameter fluctuates from 2 to 100 nm [15, 16].

CNTs are generally synthesized by three techniques: chemical vapor deposition using hydrocarbon sources (CO, methane, ethylene, acetylene), electric-arc discharge method using arc-vaporization with two carbon rods, or laser ablation method using graphite [17]. To remove CNTs impurities like amorphous carbon, fullerenes, and transition metals (used as catalysts in their synthesis), a purification step is subsequently performed by acid refluxing, surfactant aided sonication, or air oxidation methodologies [18, 19].

Combining CNTs structural dimensions with their exceptional characteristics makes them one of the most potential nanomaterials for biomedical applications [20, 21]. Their unique electrical and optical features make CNTs highly sensitive when exposed to biomolecules, leading to their

successful application as sensing components for biosensors to detect proteins, cells, or microorganisms [22]. Photoluminescence is another important characteristic of CNTs [23], which, together with their strong optical absorption in the near-infrared region [24] and Raman scattering [25], allow the CNTs orientation and quantification monitoring in biological media, highly interesting for medical imaging. Their cylindrical graphitic structure and  $sp^2$  character give them excellent mechanical properties, translating into their high strength and stiffness [26]. CNTs also possess an exceptional tensile force, turning them into a robust product with improved thermal conductivity [26]. Notably, the effective possibility of functionalized CNTs to incorporate molecules, namely proteins, and their ability to cross biological barriers, like the cell membrane and penetrate individual cells [27], enable them to act as effective drug carriers [28]. Several authors reported a more effective and safer administration of drugs into cells when bonded to CNTs than by traditional techniques [18, 19]. This function allows overcoming the problems associated with several medications, like low solubility, faster deactivation, and limited bioavailability [29]. The possibility of internalization and release of CNTs from cells, along with their incomparable photothermal response, allows their use as photothermal therapeutic agents to reduce tumor size or even to destroy cancer cells by near-infrared laser irradiation [30, 31].

Despite their relevance in this field, the biomedical application of CNTs raises some questions about safety and potential cytotoxicity issues. Intending a safe CNTs use, high purity CNTs are preferred to limit potential toxic ions release during the application. However, this can be a real challenge on a large scale, having to reach a compromise between quality and quantity [32]. The CNTs toxicity has been a hot topic of discussion, with many publications but without a clear conclusion.

This book chapter overviews the potential applications of CNTs in the biomedical sector, highlighting their usage on diagnosis and devices, tissue engineering, delivery systems, and target therapies (**Figure 1**). Particular attention is also given to the CNTs potential toxicity, and attempts to overcome this issue.

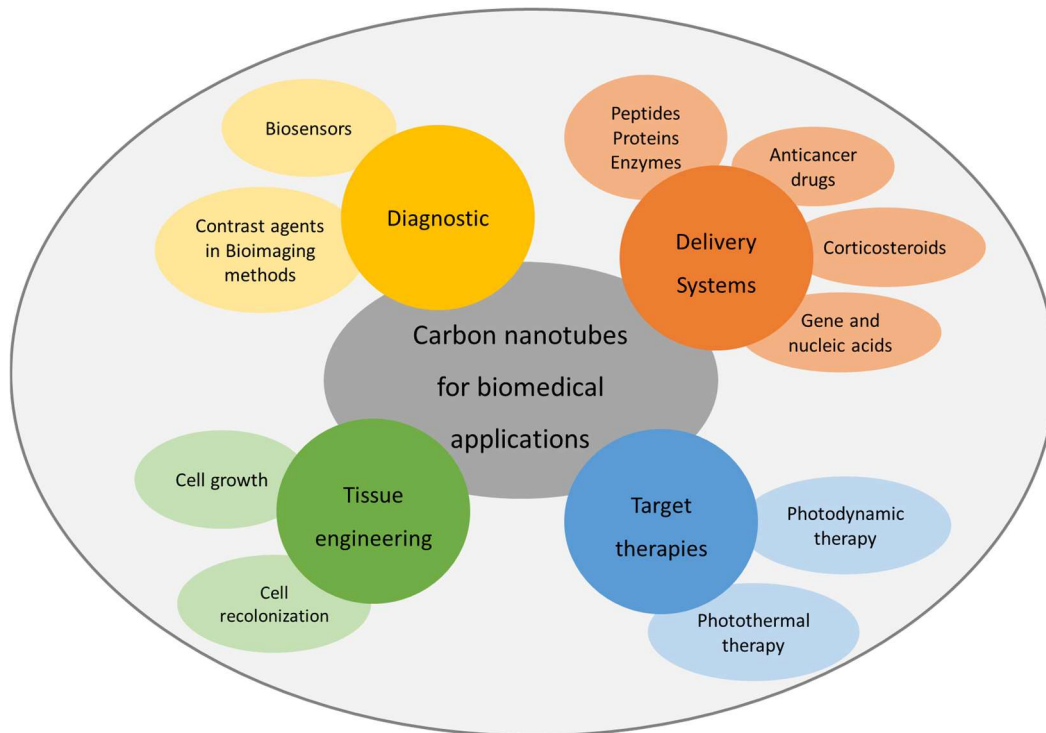


Figure 1. Scheme summarizing the biomedical applications of carbon nanotubes overviewed in this book chapter.

## 2. Carbon nanotubes in biomedical applications

### 2.1. Carbon nanotubes in diagnostic

The success of disease treatment is majorly based on early diagnostic and improved detection methods [32]. In this sense, several technologies based on CNTs have been developed to improve the diagnostic and detection methods. Due to their electronic properties, CNTs have been considered the key element of electrochemical sensors, and different kinds of label-free CNT-based biosensors were developed [32, 33]. Additionally, CNTs can act as contrast agents in other bioimaging methods [32, 34].

#### 2.1.1. Carbon-nanotubes-based biosensors

Biosensors are analytical devices that combine a biological component and a physicochemical detector to identify a target analyte [15]. CNTs-based biosensors are modern devices, while representing an exciting application area for *in vitro* and *in vivo* diagnostics and therapeutic monitoring, namely diabetes and bacterial infections [32]. Due to their length scale and unique structure, the use of CNTs-based biosensors is highly recommended for sensitive diagnostics and

analyses, from laboratory to clinic applications. Specifically, CNT-based biosensors can be used for the detection of several biological structures, such as glucose, antigens, viruses, DNA (deoxyribonucleic acid), reactive oxidative species (ROS), and even whole cells, providing a fast and straightforward solution for molecular diagnosis (**Figure 2**) [15].

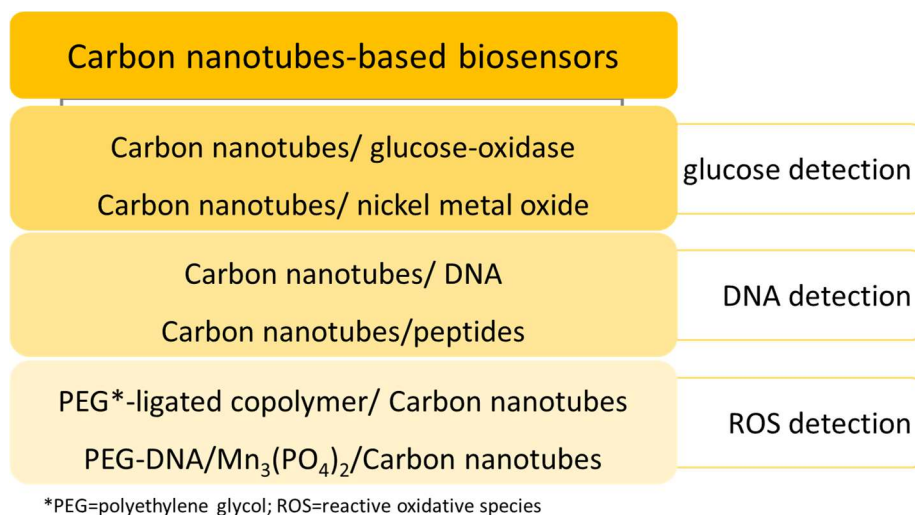


Figure 2. Carbon-nanotubes-based biosensors used in the detection of several biological structures.

Several researchers have been developed CNT-based biosensors by coupling CNTs with glucose-oxidase for blood sugar detection (**Table 1**). Zhou et al. [35] developed a glucose CNT-based biosensor through the covalent linkage of ferrocene-grafted dendrimer on the surface of CNTs-chitosan nanocomposite modified electrode able to immobilize a high-content of glucose oxidase (CNTs-CHI/dendrimerFc/GOx). Due to the excellent electron transfer acceleration of CNTs and the high loading content of the glucose oxidase and ferrocene mediator on the electrode matrix, this biosensor showed excellent analytical performance, with a fast response time of less than 10 s, a wide linear range from 0.02 to 2.91 mM and low detection limit down to 7.5  $\mu\text{M}$  [35]. Shrestha et al. [36] developed a highly electroactive bio-nanohybrid film of polypyrrole-Nafion-functionalized MWCNTs nanocomposite prepared on the surface of glassy carbon electrode (PPy-Nf-fMWCNTs) by an easy one-step electrochemical polymerization technique followed by chitosan-glucose oxidase immobilization on its surface. This MWCNT-based biosensor revealed an improved sensitivity ( $2860.3 \mu\text{A mM}^{-1} \text{cm}^{-2}$ ), low detection limit (5  $\mu\text{M}$  under a signal/noise ratio of 3), long-term stability, good repeatability, reproducibility, and acceptable measurement of glucose concentration in real serum samples [36]. Using gold nanoparticles decorated MWCNTs, Devasenathipathy et al. [37] similarly prepared a CNT-based biosensor (GR-MWCNTs/AuNPs) for the determination of glucose. Biopolymer pectin stabilized gold nanoparticles were prepared at graphene and MWCNTs, where glucose oxidase was



successfully immobilized. The manufactured glucose biosensor showed two linear ranges: 10  $\mu\text{M}$  – 2 mM with a limit of detection of 4.1  $\mu\text{M}$ , and 2 mM – 5.2 mM with a limit of detection of 0.95 mM. Moreover, the biosensor exhibited appreciable stability, repeatability, reproducibility, and practicality. Comparing the biosensor performance with other reported sensors revealed a significant improvement in the overall sensor performance [37]. On the other hand, Zhang et al. [38] described a non-enzymatic glucose detector composed of a porous nickel-based metal oxide framework (Ni-MOF/CNTs), where the addition of CNTs enhanced the electrical conductivity. These electrodes exhibited a low detection limit (0.82  $\mu\text{M}$ ), a high sensitivity of 13.85 mA mM<sup>-1</sup>cm<sup>-2</sup>, a wide linear range from 1  $\mu\text{M}$  to 1.6 mM, and a good reproducibility and repeatability. In this sense, the proposed sensor is found as a relevant alternative for glucose detection through immune complexes immobilization [38].

Other promising CNT-enzyme biosensors, such as CNT-based dehydrogenase biosensors [39] or peroxidase [40] biosensors, have been developed for different therapeutic monitoring and diagnostics. Beyond CNT-based biosensors for blood sugar detection, CNT-based biosensors to detect DNA have been prepared. For example, He et al. [41] developed a CNT-DNA-based biosensor by modifying CNTs with single-strand DNA chains. A gold-supported aligned CNT array was firstly treated with acetic acid. Then, single-strand DNA chains with an amino group were chemically bonded with the plasma-induced eCOOH group on the CNTs via amide formation. Finally, ferrocenecarboxaldehyde was labeled to complementary DNA chains and other non-complementary DNA chains. This CNT-DNA-based biosensor exhibited a high selectivity and sensitivity for probing complementary DNA and target DNA chains of specific sequences [41]. Recently, Li et al. [42] developed a CNT-based biosensor for DNA recognition through a bio-interaction between DNA and biomolecules. A CNT-peptide-based biosensor was prepared using the peptide (with the sequence Fmoc-RRMEHRMEW) discovered by the authors, and which has a special bio-interaction with tiny nucleic acids and causes a significant decrease in zeta potential. Compared to the former reported universal DNA bio-detector and NanoDrop (a spectrometer from Thermo Scientific™), this unique CNT-peptide-based DNA biosensor demonstrated a broader sensing range (from  $1.6 \times 10^{-4}$  to 5  $\mu\text{mol L}^{-1}$ ) and a significantly lower detection limit (0.88  $\mu\text{g L}^{-1}$ ) [42].

CNTs have been also used *in vivo* biosensing. Sudibya et al. [43] prepared CNT-based biosensors by the functionalization of CNTs with bioactive monosaccharides. The authors demonstrated that the CNT-monosaccharides-based biosensor could interact with living cells surface and dynamically detect biomolecules [43]. Additionally, Hu et al. [44] reported a CNT-based biosensor through the functionalization of CNT/polyethylene with DNA and Mn<sub>3</sub>(PO<sub>4</sub>)<sub>2</sub>, and detected ROS *in situ* released from cancer cells under drug stimulations. Living human breast

carcinoma cells (MDA-MB-231) can grow on the CNT/polyethylene-DNA/Mn<sub>3</sub>(PO<sub>4</sub>)<sub>2</sub> biosensor forming an MDA-MB-231/Mn<sub>3</sub>(PO<sub>4</sub>)<sub>2</sub>/DNA-polyethylene/CNT hybrid film, creating a very short diffusion distance between cells and reaction sites, resulting in a highly sensitive method (detection limit of  $30 \times 10^{-9}$  M and sensitivity of 9.6 and 20.8  $\mu\text{A } \mu\text{M}^{-1} \text{cm}^{-2}$  depending on the linear range) for detecting ROS. Jin et al. [45] developed a CNT-based biosensor to detect ROS, namely single-molecules of H<sub>2</sub>O<sub>2</sub>, using fluorescent SWNTs, and found that epidermal growth factor induces 2 nmol H<sub>2</sub>O<sub>2</sub> locally for 50 min. For the detection of local nitric oxide, Iverson et al. [46] have modified near-infrared fluorescent SWNTs with a polyethylene glycol-ligated copolymer, enabling intravenous injection into mice and the selective detection of nitric oxide concentration (detection limit of 1  $\mu\text{M}$ ) with no intrinsic immune reactivity or other adverse response for more than 400 days. The half-life for liver retention is 4 h, with sensors clearing the lungs within 2 h after injection, thus avoiding a dominant route of *in vivo* nanotoxicology. After localization within the liver, it was possible to follow the transient inflammation using nitric oxide as a marker and signaling molecule [46].

Table 1. Examples of developed CNTs-based biosensors used in the detection of several biological structures and main results.

	Biosensor	Main Results	Reference
Glucose detection	<b>CNTs-CS/dendrimerFc/GOx</b> Ferrocene-grafted dendrimer covalently linked on the surface of CNTs-chitosan nanocomposite modified electrode	<ul style="list-style-type: none"> <li>fast response time (less than 10 s)</li> <li>wide linear range (from 0.02 to 2.91 mM)</li> <li>low detection limit (down to 7.5 <math>\mu\text{M}</math>)</li> </ul>	[35]
	<b>PPy-Nf-fMWCNTs</b> Bio-nanohybrid film of polypyrrole-Nafion-functionalized MWCNTs nanocomposite prepared on the surface of glassy carbon electrode	<ul style="list-style-type: none"> <li>improved sensitivity (<math>2860.3 \mu\text{A mM}^{-1}\text{cm}^{-2}</math>)</li> <li>low detection limit (5 <math>\mu\text{M}</math> under a signal/noise ratio of 3)</li> <li>long-term stability</li> <li>good repeatability and reproducibility</li> <li>acceptable measurement of glucose concentration in real serum samples</li> </ul>	[36]
	<b>GR-MWCNTs/AuNPs</b> Biopolymer pectin stabilized gold nanoparticles prepared in MWCNTs	<ul style="list-style-type: none"> <li>Two linear ranges: 10 <math>\mu\text{M}</math> – 2 mM with a limit of detection of 4.1 <math>\mu\text{M}</math> 2 mM – 5.2 mM with a limit of detection of 0.95 mM</li> <li>Appreciable stability, repeatability, reproducibility, and practicality</li> </ul>	[37]
	<b>Ni-MOF/CNTs</b> Nickel-based metal organic framework linked to functional CNTs	<ul style="list-style-type: none"> <li>Low detection limit (0.82 <math>\mu\text{M}</math>)</li> <li>High sensitivity (<math>13.85 \text{ mA mM}^{-1}\text{cm}^{-2}</math>)</li> <li>Linear range (1 <math>\mu\text{M}</math>–1.6 mM)</li> <li>Good reproducibility and repeatability</li> </ul>	[38]
DNA detection	<b>Gold-supported CNTs – DNA sensors</b>	<ul style="list-style-type: none"> <li>High selectivity and sensitivity</li> </ul>	[41]

<b>ROS detection</b>	<b>CNTs – peptide (Fmoc-RRMEHRMEW)</b>	<ul style="list-style-type: none"> <li>• Broader sensing range (<math>1.6 \times 10^{-4}</math> to <math>5 \mu\text{mol L}^{-1}</math>)</li> <li>• Low detection limit (<math>0.88 \mu\text{g L}^{-1}</math>)</li> </ul>	[42]
	<b>CNTs/polyethylene-DNA/Mn<sub>3</sub>(PO<sub>4</sub>)<sub>2</sub></b>	<ul style="list-style-type: none"> <li>• Low detection limit (<math>30 \times 10^{-9}</math> M)</li> <li>• High sensitivity (<math>9.6</math> and <math>20.8 \mu\text{A } \mu\text{M}^{-1} \text{cm}^{-2}</math>)</li> </ul>	[44]
	<b>Fluorescent SWNTs</b>	<ul style="list-style-type: none"> <li>• Detection of single-molecules of H<sub>2</sub>O<sub>2</sub></li> </ul>	[45]
	<b>Fluorescent SWNTs/polyethylene glycol-ligated copolymer</b>	<ul style="list-style-type: none"> <li>• Selective detection of nitric oxide concentration</li> <li>• Low detection limit (<math>1 \mu\text{M}</math>)</li> <li>• No immune reactivity or other adverse response (for more than 400 days)</li> </ul>	[46]

### 2.1.2. Imaging methods using carbon nanotubes

Standard diagnostic techniques for monitoring and detect the tissue regeneration process in small animals, namely histology analysis that is the most robust diagnostic technique, lead to significant variation results and difficult the assessments of temporal results in a statistically significant manner. In this sense, and taking advantage of intrinsic properties of CNTs, different CNTs-based materials have been developed for applications in a multiplicity of imaging modalities, such as photoluminescence imaging through near-infrared fluorescence, photoacoustic tomography, Raman spectroscopy, magnetic resonance, and radionuclide-based imaging, offering scientists a piece of spatial and temporal information in a faster and more convenient manner (**Figure 3**) [47].

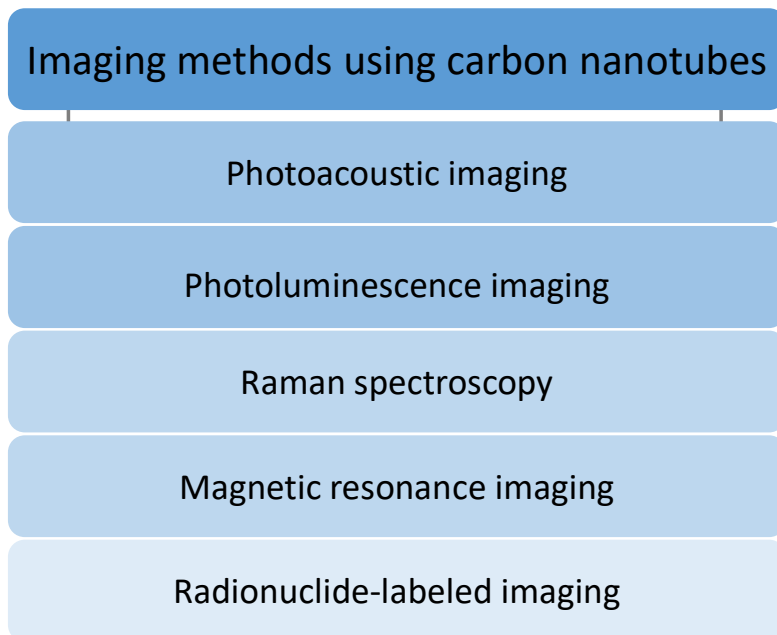


Figure 3. Imaging modalities where CNTs have been applied.

In photoluminescence imaging, SWCNTs are excited emitting fluorescence in the near-infrared-I (700–900 nm) and near-infrared-II (1100–1400 nm) ranges, where tissues and water are almost transparent, making it possible to reach deeper penetration depths. In fact, SWCNT fluorescence was emerging as a reliable optical imaging method for vessel observation and used as an alternative optical method to the expensive positron emission tomography-computed tomography for brown fat detection [32]. Welscher and co-authors [48, 49] used this property to optically detect in real-time the biodistribution of injected SWCNTs in mice deep tissues and vessels. The authors synthesized phospholipid-polyethylene glycol-coated SWCNTs by sonicating SWCNTs with sodium cholate, followed by surfactant exchange. They used these materials as *in vivo* near-infrared photoluminescence imaging agents for live mice. The high-

resolution intravital image of tumor vessels beneath thick skin was achieved due to deep tissue penetration and low autofluorescence background. Cherukuri et al. [50] also used near-infrared fluorescence microscopy to image SWCNTs in macrophage cells. Macrophage samples were incubated in growth media with SWCNTs at different concentrations to track their *ex vivo* uptake in mouse peritoneal macrophage cells. Near-infrared fluorescence imaging revealed no difference in population growth, adhesion, morphology, and confluence between the control and the cultures containing SWCNTs, and the SWCNTs uptake appears to occur through phagocytosis. Additionally, Leeuw et al. [51] have used *in vivo* near-infrared imaging to assess the biocompatibility of SWCNTs in an intact organism, *Drosophila melanogaster*. This study showed the effectiveness of SWCNTs as near-infrared probes for studying individual nanotubes in tissue specimens or inside living organisms during tissue regeneration. Based on all these studies, photoluminescence imaging seems to be a promising method for tracking SWCNTs in cells and small animals over long durations of time.

Beyond photoluminescence, the photoacoustic effect is another attractive way to use CNT near-infrared absorption. Photoacoustic imaging measures the ultrasounds produced by tissue expansion and heat emitted by CNTs exposed to near-infrared stimulation [32]. Improved contrast on targeted tumor cells, using SWCNTs conjugated with Arginine-Glycine-Aspartate peptides as well as an enhanced sensitivity and detection threshold, was obtained to pristine SWCNT [52, 53]. SWCNT was reported as a technique that differentiates multipotent marrow stromal cells (MSCs) toward osteoblasts [54]. It was demonstrated that a brief (10 min) daily nanoparticle-facilitated exposure of MSCs to nanosecond pulse laser-induced photoacoustic stimulation enhanced differentiation [54].

Raman scattering is also an imaging option due to the vibrational and low-frequency modes of CNTs based on inelastic scattering, which appears at 1,590–1,600  $\text{cm}^{-1}$  (G band, due to stretching along the C–C bond of graphene). Resonance-enhanced Raman bands for SWCNTs appear at 150–300  $\text{cm}^{-1}$  (radial breathing modes), which can be related to the diameter of the SWCNTs [32, 55]. Thus, Raman imaging allows for the spatial and chemical imaging of SWCNTs in cells and small animals. Heller et al. [56] applied Raman spectroscopy to monitor cells labeled with CNTs. These nanotube aggregates remained in the cell and displayed scattering even after several cycles of cell division, showing potential as markers in assessing the proliferation and differentiation of cells in culture, long-term labeling of cell populations, and continuous monitoring of the cellular environments [56]. Raman imaging was also applied in study biodistribution and blood circulation of PEGylated SWCNTs in a mouse model [57]. The results showed SWCNT accumulation in the intestine, feces, kidney, and bladder of mice and suggested excretion and clearance of SWCNTs from mice via the biliary and renal pathways [57]. Another

study indicated Raman imaging for real-time monitoring of SWCNTs for disease (tumor) targeting [58]. Specifically, disease targeting SWCNTs (RGD–SWCNT, arginine–glycine–aspartic acid peptides) were examined for localization in diseased (tumor) mice as against plain SWCNT [58]. The images showed a higher accumulation of RGD–SWCNTs in the tumor than the non-functionalized SWCNT mouse group, with a lower accumulation in the liver and spleen [58].

CNTs have also been shown to increase the contrast enhancement efficacy of metal ions, such as gadolinium, commonly applied in magnetic resonance imaging as a contrast agent [59]. Magnetic resonance imaging is a non-invasive imaging modality regularly used to diagnose several diseases and physio-chemical states of tissue and blood flow since it provides anatomical details [60]. In magnetic resonance imaging it is applied an external magnetic field and radiofrequency pulses, exciting proton spin states. From the excited state spin to equilibrium is required a period, the relaxation time. This relaxation causes a change in the flux of the receiving coil of the magnetic resonance imaging scanner, inducing a magnetic resonance signal. The relaxation time affects the quality of the image, especially the contrast [60]. Contrast agents, such as gadolinium, are used to improve the contrast since they can modulate the relaxation time. Sitharaman et al. [61] reported the use of SWCNTs as carriers of gadolinium. The authors described the encapsulation of  $Gd^{3+}$  ions with SWCNTs to sequester the toxic effect of  $Gd^{3+}$  ions and amplify the contrast-enhancing efficacy. The results showed an increase in proton relaxation time, increasing the contrast and enhancing the efficacy [61]. Therefore, GB-SWCNT-based magnetic resonance imaging contrast agents could be dispersed throughout an engineered tissue, and for instance, to monitor the process of tissue regeneration [61].

Efficient contrast agents were also developed by functionalizing MWCNTs with gadolinium chelating agent, diethylene triamine penta-acetic acid, enabling tight attachment of gadolinium (Gd) atoms onto the nanotube surface [59]. The resulting Gd-MWNTs contrast agents were found to be three times better than the clinically approved T1 contrast agent Magnevist. Moreover, the Gd-MWNTs contrast agents were stable over two weeks in water and mouse serum [59]. The functionalization method used by Servant and co-workers [59] was previously applied by Radioprobes composed of metal halides ( $Na^{125}I$ ), encapsulated within SWCNTs, were developed for single-photon emission computed tomography imaging, another application of CNTs in bioimaging [62]. In brief, metal halides were sealed inside SWCNTs to create high-density radio-emitting crystals, while SWCNTs surfaces were then covalently sealed with biantennary carbohydrates, improving dispersibility and biocompatibility. The intravenous administration of these radio probes in mice was tracked *in vivo* using single-photon emission computed tomography imaging, resulting in ultrasensitive imaging and delivery of unprecedented radio dose density [62].

Beyond the examples of CNT-based contrast agents on studies that harness the intrinsic properties of these nanomaterials, different investigations have shown that only functionalization of the external carbon sheath of CNTs (SWCNTs or MWCNTs) with appropriate imaging agents allows molecular imaging [63, 64].

## **2.2. Carbon nanotubes in tissue engineering**

Tissue engineering combines biological and material sciences, in which the fast development of nanotechnology and nanomaterials is an opportunity to enhance biomedical engineering. CNTs present several and very distinct properties, can be assembled into different morphologies, such as fibers, films, and three-dimensional (3D) structures, and have a positive influence on living cells. All these properties make of these nanomaterials suitable for tissue engineering [32, 65]. Several authors have described promising results in this field, with Lovat et al. [66] reporting CNTs as a good surface for cellular growth and as potential devices able to improve neural signal transfer while supporting dendrite elongation and cell adhesion. It was demonstrated the growth of neuronal circuits on a CNT grid accompanied by a significant increase in the network activity, which may be related to the specific properties of CNT materials, such as the high electrical conductivity [66].

Mazzatenta and co-authors [67] developed an integrated SWCNT–neuron system to investigate whether electrical stimulation delivered via SWCNTs can induce neuronal signaling. To this end, hippocampal cells were grown on pure SWCNT substrates and patch clamped, and neuronal responses to voltage steps delivered either via conductive SWCNTs substrates or via the patch pipette were compared. The results, also supported by mathematical models, revealed that SWCNTs could directly stimulate brain circuit activity, highlighting SWCNTs as a promising material [67]. Similarly, it was proved that neurons would preferentially grow on thin layers of double-walled carbon nanotubes (DWCNTs) compared to SiO<sub>2</sub> surface, possibly explained by a favorable surface texture and better adsorption of culture medium proteins, allowing patterning of neurons networks [68]. Additionally, cell differentiation was also enhanced when the growth occurred on DWCNTs [68]. The success of pristine MWCNTS was reported in the growth and proliferation of pancreatic cancer cells, exhibiting a new approach to studying this kind of cancer [69]. Due to the ability of CNTs to form 3D architectures, MWCNT-based 3D networks as scaffolds for cell growth were developed [70]. The 3D interlocking resistive network of MWCNTs was prepared by treating a vertically aligned MWCNT array with exerting chemically induced capillary forces [70]. The proposed MWCNT-based 3D networks could be shaped to fit the best natural tissue morphology but also remained stable *in vivo*. Seven days later fibroblasts had covered entirely almost the whole surface of the MWCNT-based 3D scaffolds [70].



For regenerative purposes, drugs or biofunctional molecules have been delivered by CNT-based 3D porous scaffolds to control their release profile and specific interactions with the attached cells [71]. The common strategy is to bind proteins, such as growth factors or enzymes onto functionalized CNTs [71]. MWCNT/chitosan composite scaffolds were prepared to support cell recolonization [72]. Scaffolds were composed of MWNTs (up to 89%) and chitosan. These MWNT/chitosan composite scaffolds showed a remarkable biocompatible character in both *in vitro* and *in vivo* experiments. The authors also investigated the evolution of a cell line toward an osteoblastic lineage in the presence of the recombinant human bone morphogenetic protein-2 (rhBMP-2) *in vivo* [72]. The results obtained are based on rhBMP-2-adhered MWNT/chitosan scaffolds used into subcutaneous pockets in the mouse back muscle tissue for 3 weeks [72]. After this time, most of the MWNT/chitosan scaffold structure was degraded and replaced by cells, and bone tissue regeneration was clearly observed [72]. A fibronectin/CNT hybrid was also produced, and it was found that fibronectins maintained their native structures upon CNT binding [73]. The hybrid material displayed a stronger affinity to human mesenchymal stem cells than the conventional fibronectin coated glass. Selective and accelerated growth of the cells was also demonstrated on the patterned fibronectin/CNT hybrid nanostructures [73].

CNTs have been applied in nerve tissue engineering, namely by investigating the growth and organization of neural networks to treat neural diseases. Keefer et al. [74] prepared CNTs coated with conventional tungsten and stainless steel wire electrodes using electrochemical techniques under ambient conditions. The CNTs coating enhanced both recording and electrical stimulation of neurons in culture, rats, and monkeys by decreasing the electrode impedance and increasing charge transfer. Similarly, platinum/tungsten microelectrodes coated with a polypyrrole-CNT composite were reported as responsible for significantly reducing microelectrode impedance at all neuronal signal frequencies and an improvement of the signal-to-noise ratio [75]. Lee et al. [76] pre-treated rats with amine-modified SWNTs and found that the pre-treatment can protect neurons and enhance the recovery of behavioral functions in rats with induced stroke. Less tissue damage was observed in SWNT-treated rats than in controls. To understand the mechanisms in which CNTs might affect the activity of cultured neuronal networks, single-cell electrophysiology techniques, electron microscopy analysis, and theoretical modeling were applied [77]. It was showed that CNTs improved the responsiveness of neurons by forming tight contacts with the cell membranes that might favor electrical shortcuts between the proximal and distal compartments of the neuron [77].

## 2.3. Carbon Nanotubes in Delivery Systems

All types of active molecules can be potentially linked to functionalized CNTs (fCNTs), allowing their application in drug, gene, and vaccine delivery [78, 79]. In fact, fCNTs are broadly applied as a delivery tool of therapeutic agents, namely anticancer drugs, antihypertensive drugs, corticosteroids, genes and nucleic acids, proteins, enzymes, peptides, ligands to their specific sites [80, 81] (Figure 4).

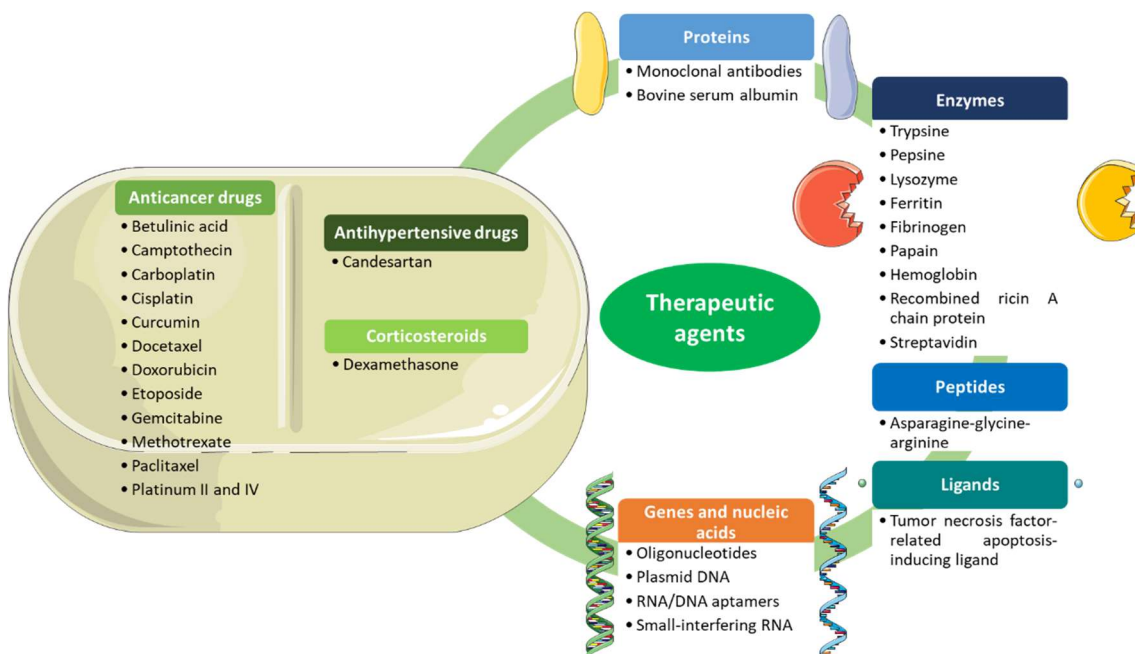


Figure 4. Therapeutic agents applied in delivery systems using functionalized carbon nanotubes.

### 2.3.1. Anticancer drugs, antihypertensive drugs, and corticosteroids

Drug delivery systems (DDS) are tools allowing the introduction of therapeutics agents in the body through a targeted and controlled release, improving their efficacy and safety [82]. Regarding DDS with anticancer drugs linked to CNTs (Table 2), Tan et al. [83] developed a betulinic acid-oxidized MWCNTs (BA-MWCNTs) nanocomposite through a 14.5%–14.8% (w/w) loading of BA (low water-soluble drug) in MWCNT, while keeping its tubular structures. Along 22 h, 98% of BA was released using phosphate-buffered saline (PBS) solution at pH 7.4. Following 72 h, BA-MWCNTs ( $<50 \mu\text{g mL}^{-1}$ ) showed no cytotoxicity for mouse embryo fibroblast cells. Nevertheless, BA-MWCNTs displayed anticancer activity against human lung and liver cancer cell lines, revealing a half-maximal inhibitory concentration of 2.7 and 11.0  $\mu\text{g mL}^{-1}$ , respectively [83]. Additionally, Tian et al. [84] designed camptothecin-functionalized MWCNTs (CPT-fMWCNTs) supramolecular complexes via the attachment of a non-water-soluble anticancer drug (CPT) onto MWCNTs previously coated with Pluronic P123, a tri-block copolymer, through noncovalent  $\pi$ -stacking interaction to enhance its solubility. While fMWCNT only presented 10%

of antitumor activity, CPT-fMWCNTs showed around 37% of antitumor activity for HeLa cell lines [84].

The platinum (Pt)-based anticancer drug carboplatin (CP) was successfully loaded onto CNTs, as demonstrated by Arlt et al. [85], reaching a loading yield of 0.20 mg per mg of material. CP-CNT continuously released up to 68% of its Pt load within 14 days, allowing its use for drug storage. CP-CNT impaired up to 76%-94% of the clonogenic survival of prostate carcinoma (DU145, PC-3), bladder carcinoma (EJ28), and renal cell carcinoma (A498) cells. Whereas free CP simply induced 12% and 30% of apoptosis against DU145 cells, CP-CNT induced nearly 24% and 58% using  $2.5 \mu\text{g mL}^{-1}$  and  $5.0 \mu\text{g mL}^{-1}$ , respectively [85]. Moreover, Guven et al. [86] encapsulated cisplatin (CDDP), a broadly used anticancer drug, into ultra-short SWCNTs, whose coating with the surfactant, Pluronic-F108, allowed a slow, controlled CDDP release upon dialysis in PBS at  $37^\circ\text{C}$  and a higher cytotoxicity against breast cancer (MCF-7, MDA-MB-231) cell lines than free CDDP following 24 h [86].

Singh et al. [87] developed curcumin-CHI-ALG-SWCNTs through the loading of the hydrophobic anticancer drug curcumin, within SWCNTs, previously functionalized with polysaccharides, namely alginate (ALG) and chitosan (CHI), enabling a good drug loading performance and constant drug release. Treatment of human lung cancer (A549) cells with this DDS displayed enhanced cytotoxicity than free curcumin at analogous dosage, while presenting dose-related apoptotic induction [87].

Regarding DDS with docetaxel (DTX), carboxylated and acylated MWCNTs coated or covalently attached with D- $\alpha$ -Tocopherol polyethylene glycol 1000 succinate (TPGS), plus loaded with DTX and fluorescent coumarin-6 via the nano-extraction technique was reported [88]. A drug encapsulation efficiency of up to 76%, with an  $\text{IC}_{50}$  value reduction of 80-fold compared with commercial DTX injection (Docel™), was obtained with A549 cells after 24 h of incubation [88]. Following 72 h in PBS (pH 7.4), 45  $\mu\text{g}$  to 102  $\mu\text{g}$  of DTX were released, which could generate an anti-cancer impact since those concentrations are superior to their  $\text{IC}_{50}$ . DTX-TPGS-MWCNT presented substantially superior cytotoxicity, early or late apoptosis, apoptotic cell death percentage, besides minimal ROS generation and toxicity [88]. Singh et al. [89] showed carboxylated MWCNTs also loaded with TPGS and DTX, later covalently linked with transferrin (Tf), reached a similar drug encapsulation efficiency (up to 74.9%) and a DTX continuous release throughout 72 h. However, DTX-MWCNTs-Tf displayed enhanced cytotoxicity, with an  $\text{IC}_{50}$  value reduction up to 136-fold than Docel™, following 24 h incubation against A549 cells. DTX-MWCNTs-Tf presented augmented apoptotic cell death percentage, with nearly all cells in early or late apoptotic stage using a 100-fold lower DTX concentration ( $0.25 \mu\text{g mL}^{-1}$ ) than Docel™ ( $25 \mu\text{g mL}^{-1}$ ), while exhibiting low ROS levels, thus showing its efficacy and safety [89]. In the same

line, Singh et al. [90] showed that DTX/coumarin-6 loaded chitosan-folate (CHI-F) conjugated MWCNTs reached a slightly higher drug encapsulation efficiency (up to 79%), as well as attained an IC<sub>50</sub> value reduction up to 89-fold than Docel™, after 24 h incubation with A549 cell lines. Furthermore, DTX-CHI-F-MWCNTs exhibited internalization into cancer cells via a folate receptor-mediated endocytic route, substantially increased cytotoxicity and reduced toxicity, confirming its potential for targeted lung cancer treatment [90].

Concerning the use of the anticancer drug doxorubicin (DOX) in DDS, a hyaluronic acid-MWCNT (HA-MWCNT) conjugate loaded with DOX through  $\pi$ - $\pi$  stacking interaction was developed. DOX-HA-MWCNT showed a 3.2 times superior cytotoxicity, plus improved apoptotic activity than free DOX in similar concentrations [91]. The conjugate displayed a 5 times higher tumor-growth inhibitory impact than free DOX in similar concentrations, while lacking detectable cardiotoxicity, hepatotoxicity, and nephrotoxicity in mice [91]. Multiple functionalization of oxidized SWCNTs with DOX, fluorescein-labeled bovine serum albumin (BSA), and a monoclonal carcinoembryonic antigen (CEA) antibody was also displayed at non-competing binding sites [92]. The cellular uptake of DOX-BSA-CEA antibody-SWCNTs with consequent DOX translocation to the nucleus was enabled, whereas the SWCNTs remained in the cytoplasm of WiDr colon cancer cells [92]. SWCNTs coated with DOX via hydrazone linkage were also used for DDS, which was successfully taken up by liver cancer (HepG2) cells leading to enhanced cytotoxicity [93]. Polysaccharides ALG and CHI DDS were used to functionalize SWCNTs, along with the targeting promoter FA and DOX, which enabled pH-triggered DOX release, consequent nucleus penetration, and induction of HeLa cells death [94]. DDS consisting of DOX loaded onto poly(amidoamine) dendrimers altered with fluorescein isothiocyanate (FI) and FA covalently coupled to fMWCNTs attained a drug encapsulation efficiency up to 97.8%, besides allowing a pH-triggered DOX release and enhanced cytotoxicity against human epithelial carcinoma (KB) cells [95]. DOX-MWCNTs also led to increased cytotoxicity against MCF-7 cells [96].

DDS based on DOX loading of MWCNTs functionalized with poly(acrylic acid) conjugated with iron oxide magnetic nanoparticles (MNs) and coupled with FA enabled double targeted DOX delivery via a magnetic field, plus ligand-receptor interactions [97]. DOX-FA-MN-MWCNT displayed high DOX loading efficiency, as well as increased cytotoxicity toward human glioblastoma (U87) cells [97]. DOX-FA-MN-MWCNT was internalized by U87 cells with consequent intracellular DOX release and transport into the nucleus, whereas the nanoparticles remained in the cytoplasm [97]. DDS, including DOX, loaded onto the surface of SWCNTs, previously coated by FA-terminated polyethylene glycol (FA-PEG) via adsorption, reached an extremely high loading efficiency (149.3±4.1%) [98]. DOX-FA-PEG-SWCNTs showed negligible cytotoxicity against normal (3T3) cells, whereas selectively entered HeLa cells via clathrin-

mediated endocytosis, where DOX was released due to the acidic pH, subsequently entered the nucleus, thus causing cell death via transcription inhibition [98]. The association between noninvasive magnetic resonance imaging plus specific magnets positioning was reported [99]. Improved DOX loaded anti-CD105 conjugated magnetic SWCNTs targeting lung metastatic sites in a breast cancer animal model was obtained, showing its potential in cancer treatment efficiency at early plus late phases of cancer progression [99]. Besides, it was shown that DOX loaded onto dexamethasone (DEX) conjugated fMWCNTs (DEX-fMWCNTs) attained high loading efficiency ( $92.6 \pm 0.5\%$ ) while displaying low hemolyticity, plus higher cytotoxicity against A549 cells, suggesting DOX-DEX-fMWCNTs as a promising carrier for future cancer therapy [100]. The nanocomplex DOX-PEI-B-MWCNTs-siRNA (polyethyleneimine (PEI) covalently coupled with betaine (PEI-B) and MWCNTs and combined with DOX and survivin siRNA) were able to co-deliver DOX and siRNA into A549 cells, leading to the increase of the apoptotic index [101]. DOX-PEI-B-MWCNTs-siRNA reduced the tumor volume in nude mice with A549 tumor cells without causing any damages to normal tissues, confirming its potential for codelivery of anticancer drugs, as well as genes [101].

PEG-grafted MWCNTs (PEG-MWCNTs) hybrid nanosystem was used as a carrier of the lung cancer drug etoposide (VP-16) and Bcl-2 phosphorothioate antisense deoxyoligonucleotides leading to higher cytostatic efficacy, besides an enhancement of the apoptotic cells against the small cell (SCLC; DMS53) and non-small cell lung cancer (NSCLC; NCIH2135) cell lines [102].

Novel anticancer DDS, e.g., GEM-SWCNTs and GEM-PEG-SWCNTs via carboxylation, acylation, amination, and PEGylation of pristine SWCNTs followed by gemcitabine (GEM) coupling, were developed, achieving a GEM loading capacity of 43.14% (w/w) and 37.32%, respectively [103]. While GEM-SWCNTs were more cytotoxic against A549 and human pancreatic carcinoma (MIA PaCa-2) cell lines, GEM-PEG-SWCNTs presented superior efficacy in tumor growth suppression in B6 nude mice [103].

Regarding the use of methotrexate (MTX), a new theranostic prodrug, based on fMWCNTs co-tethered with MTX, a tumor targeting module (folic acid (FA)), a fluorochrome (Alexa-fluor (AF488/647)), and a radionuclide (Technetium-99m ( $^{99m}\text{Tc}$ )) was developed [104]. MTX-FA-AF-fMWCNTs were selectively internalized by folate receptor (FR) positive A549 and MCF-7 cancer cells via FR-mediated endocytosis, consequently presenting superior anticancer activity due to lysosomal trafficking [104]. The tumor-specific accumulation of MTX-FA-AF-fMWCNTs in Ehrlich Ascites tumor-bearing mice was nearly 19 and 8.6-fold superior to free MTX and MWCNTs without FA, respectively [104]. MTX-FA-AF-fMWCNTs displayed superior tumor growth arrest without showing any hepatotoxicity, cardiotoxicity, and nephrotoxicity in mice [104]. Overall, MTX-FA-AF-fMWCNTs allowed enhanced MTX therapeutic efficacy against FR positive cancer

cells, besides real-time monitoring of the treatment reaction via multimodal imaging [104]. A new MTX-CHI-MWCNT nanohybrid was developed, showing negligible toxicity against healthy (MRC-5) cells, in addition to a selective and pH-responsive MTX delivery to human lung cancer (H1299) cells [105].

A novel synergic lung cancer treatment based on the ROS-mediated cooperation between fSWCNT/graphene oxide flakes and paclitaxel (PTX) was shown to display superior cell death against NCI-H460 cells and mitogen associated protein kinase activation, as proven by the bromodeoxyuridine (BrdU) incorporation against A549 cells [106]. In addition, Sobhani et al. [107] reported MWCNTs initially functionalized with hyperbranched poly citric acid (PCA), whose carboxyl functional groups were afterward coupled with PTX shaping PTX-PCA-MWCNTs, reaching a drug encapsulation efficiency of 38% (w/w), pH-responsive PTX release into tumor tissues and cells, negligible toxicity against A549 and ovary cancer (SKOV3) cells, higher cytotoxicity than free PTX over an inferior incubation time, and enhanced cell penetration. Furthermore, PTX physically loaded via immersion of PEG-SWCNT and PEG-MWCNT exhibited a saturated PTX solution in methanol, achieved a loading capability of 26% (w/w) and 36% (w/w), respectively [108]. Both PEG-SWCNT and PEG-MWCNT displayed sustainable PTX release in buffer solution and superior efficacy against HeLa and MCF-7 cells, as shown by the  $IC_{50}$  value inferior to free PTX, suggesting its potential for cancer therapeutics [108]. The co-exposure of SWCNTs and PTX led to increased cell death and apoptosis induction of human ovarian cancer (OVCAR3) cells, implying its potential for cancer treatment progress [109]. A novel DDS PTX/HA-CHI-SWCNTs comprising CHI non-covalently linked to SWCNTs was shown to enhance biocompatibility, combined with HA connected to the outer CHI layer to provide targeting features later attached to PTX [110]. PTX/HA-CHI-SWCNTs displayed negligible toxicity toward normal fibroblast cells, and enhanced toxicity and apoptosis induction to A549 cells, showing potential for cancer therapy [110].

Feazell et al. [111] developed a Pt(IV)-fSWCNT conjugate, which successfully delivered a lethal dosage of cis-[Pt(NH<sub>3</sub>)<sub>2</sub>Cl<sub>2</sub>] upon intracellular reduction. Whereas cis-[Pt(NH<sub>3</sub>)<sub>2</sub>Cl<sub>2</sub>] was almost non-toxic, Pt(IV)-fSWCNT exhibited a substantially enhanced cytotoxicity profile against testicular carcinoma (NTera-2) cells [111]. Besides that, the properly load of CDDP or of an inert Pt(IV) complex into fMWCNTs was managed, whose administration in mice considerably augmented the Pt content in certain tissues (especially lung, liver, and spleen) while not causing inflammatory reaction or necrosis [112].

In the field of CNTs, antihypertensive drugs have also been applied in DDS (**Table 2**). The only work found showed a dual-targeting, plus co-delivery method, applying iRGD-PEI-MWCNT-SS-CD/pAT2 complexes formed by tumor-homing peptide (iRGD) attached to PEI connected to

MWCNT skeleton, combined with CD linked via cystamine (SS) to the MWCNT, all of which were assembled by plasmid AT2 (pAT2) [113]. iRGD-PEI-MWCNT-SS-CD/pAT2 complexes were designed for antiangiogenesis therapy in lung cancer, which targeted the renin-angiotensin system (RAS) dysregulation through the synergistic regulation of angiotensin II type 1 receptor (AT1R), plus type 2 receptor (AT2R) pathway. iRGD-PEI-MWCNT-SS-CD/pAT2 complexes displayed significant neovascularization and tumor growth suppression in A549 xenograft nude mice [113].

In addition to the previously described drugs, corticosteroids have also been used (**Table 2**). Komane et al. [114] showed vertically aligned (VA)-MWCNTs functionalized and PEGylated, before the loading of the anti-inflammatory glucocorticoid, led to the enhancement of its release, displaying 55%, 65%, and 95% release at pH 7.4, 6.5 and 5.5, respectively. VA-fMWCNTs (20 to 20,000  $\mu\text{g mL}^{-1}$ ) exhibited a shallow cytotoxicity effect in PC-12 cells, revealing their potential in ischemic stroke treatment [114].

Table 2. Anticancer drugs, antihypertensive drugs, and corticosteroids used in drug delivery systems with carbon nanotubes and corresponding main results.

	Therapeutic agents	Drug delivery systems	Main Results	Reference
Anticancer drugs	Betulinic acid (BA)	BA-MWCNTs nanocomposite	<ul style="list-style-type: none"> <li>• 14.5%–14.8% (w/w) BA loading</li> <li>• 98% of BA was released at pH 7.4 (along 22 h)</li> <li>• No cytotoxicity for mouse embryo fibroblast cells</li> <li>• Anticancer activity against human lung and liver cancer cell lines</li> </ul>	[83]
	Camptothecin (CPT)	CPT-fMWCNTs supramolecular complexes  Designed via the attachment of CPT onto MWCNTs previously coated with Pluronic P123, a tri-block copolymer, through noncovalent $\pi$ -stacking interaction	<ul style="list-style-type: none"> <li>• Around 37% of antitumor activity for HeLa cell lines</li> </ul>	[84]
	Carboplatin (CP)	CP-CNT	<ul style="list-style-type: none"> <li>• 0.20 mg per mg of material of loading yield</li> <li>• Continuously released up to 68% of its platinum (Pt) load within 14 days</li> <li>• Impaired up to 76%-94% of the clonogenic survival of prostate carcinoma (DU145, PC-3), bladder carcinoma (EJ28), and renal cell carcinoma (A498) cells</li> <li>• Induced nearly 24% and 58% of apoptosis against DU145 cells using 2.5 <math>\mu\text{g mL}^{-1}</math> and 5.0 <math>\mu\text{g mL}^{-1}</math></li> </ul>	[85]
	Cisplatin (CDDP)	CDDP-SWCNTs	<ul style="list-style-type: none"> <li>• Slow, controlled CDDP release upon dialysis in PBS at 37°C</li> </ul>	[86]



	CDDP encapsulation into ultra-short SWCNTs coated with the surfactant Pluronic-F108	<ul style="list-style-type: none"> <li>• Higher cytotoxicity against breast cancer (MCF-7, MDA-MB-231) cell lines than free CDDP following 24 h</li> </ul>
<b>Curcumin</b>	<p><b>Curcumin-CHI-ALG-SWCNTs</b></p> <p>Loading of curcumin, within SWCNTs, previously functionalized with polysaccharides, namely alginate (ALG) and and chitosan (CHI)</p>	<ul style="list-style-type: none"> <li>• Excellent drug loading performance and constant drug release [87]</li> <li>• Treatment of human lung cancer (A549) cells displayed enhanced cytotoxicity than free curcumin at analogous dosage while presenting dose-related apoptotic induction</li> </ul>
<b>Docetaxel (DTX)</b>	<p><b>DTX-TPGS-MWCNT</b></p> <p>Carboxylated and acylated MWCNTs coated or covalently attached with D-<math>\alpha</math>-Tocopherol polyethylene glycol 1000 succinate (TPGS), loaded with DTX and fluorescent coumarin-6 via the nano-extraction technique</p>	<ul style="list-style-type: none"> <li>• Drug encapsulation efficiency up to 76% [88]</li> <li>• IC<sub>50</sub> value reduction of 80-fold when comparing with commercial DTX injection (Docel™), following 24 h incubation with A549 cells</li> <li>• Following 72 h in PBS, 45 <math>\mu</math>g to 102 <math>\mu</math>g of DTX were released, which could generate anti-cancer impact since those concentrations are superior to their IC<sub>50</sub></li> <li>• Substantially superior cytotoxicity, early or late apoptosis, apoptotic cell death percentage, minimal ROS generation, and toxicity</li> </ul>
	<p><b>DTX-MWCNTs-Tf</b></p> <p>Carboxylated MWCNTs loaded with TPGS and DTX, later covalently linked with transferrin (Tf)</p>	<ul style="list-style-type: none"> <li>• Drug encapsulation efficiency up to 74.9% [89]</li> <li>• DTX continuous release throughout 72 h</li> <li>• Enhanced cytotoxicity, an IC<sub>50</sub> value reduction up to 136-fold than Docel™, following 24 h incubation against A549 cells</li> </ul>

		<ul style="list-style-type: none"> <li>• Augmented apoptotic cell death percentage, with nearly all cells in early or late apoptotic stage using a 100-fold lower DTX concentration (<math>0.25 \mu\text{g ml}^{-1}</math>) than Docel™ (<math>25 \mu\text{g ml}^{-1}</math>), while exhibiting low ROS levels</li> </ul>	
	<p><b>DTX-CHI-F-MWCNTs</b></p> <p>DTX/ coumarin-6 loaded chitosan-folate (CHI-F) conjugated MWCNTs</p>	<ul style="list-style-type: none"> <li>• Drug encapsulation efficiency up to 79%</li> <li>• <math>\text{IC}_{50}</math> value reduction up to 89-fold than Docel™, after 24 h incubation with A549 cell lines</li> <li>• Internalization into cancer cells via a folate receptor-mediated endocytic route substantially increased cytotoxicity and reduced toxicity</li> </ul>	[90]
<b>Doxorubicin (DOX)</b>	<p><b>DOX-HA-MWCNT</b></p> <p>Hyaluronic acid (HA)-MWCNT conjugate loaded with DOX through <math>\pi</math>-<math>\pi</math> stacking interaction</p>	<ul style="list-style-type: none"> <li>• 3.2 times superior cytotoxicity, plus improved apoptotic activity than free DOX in similar concentrations</li> <li>• 5 times higher tumor-growth inhibitory impact than free DOX in similar concentrations while lacking any detectable cardiotoxicity, hepatotoxicity, and nephrotoxicity in mice</li> </ul>	[91]
	<p><b>DOX-BSA-CEA antibody-SWCNTs</b></p> <p>Multiple functionalization of oxidized SWCNTs with DOX, fluorescein-labeled bovine serum albumin (BSA), and a monoclonal carcinoembryonic antigen</p>	<ul style="list-style-type: none"> <li>• Cellular uptake with consequent DOX translocation to the nucleus, whereas the SWCNTs remained in the cytoplasm of WiDr colon cancer cells</li> </ul>	[92]

---

(CEA) antibody at non-competing binding sites

---

**DOX-SWCNTs** • Successfully taken up by liver cancer (HepG2) cells leading to enhanced cytotoxicity [93]

SWCNTs coated with DOX via hydrazone linkage

---

**DOX-FA-CHI-ALG-SWCNTs** • pH-triggered DOX release, consequent nucleus penetration, and induction of HeLa cells death [94]

SWCNTs functionalized with the polysaccharides alginate (ALG) and chitosan (CHI), along with the targeting promoter FA and DOX

---

**DOX-FI-FA-fMWCNTs** • Drug encapsulation efficiency up to 97.8% [95]

DOX loaded onto poly(amidoamine) dendrimers altered with fluorescein isothiocyanate (FI) and FA covalently coupled to fMWCNTs

• pH-triggered DOX release and enhanced cytotoxicity against human epithelial carcinoma (KB) cells

---

**DOX-MWCNTs** • Increased cytotoxicity against MCF-7 cells [96]

---

**DOX-FA-MN-MWCNT** • High DOX loading efficiency [97]

DOX loading of MWCNTs functionalized with poly(acrylic acid) conjugated with iron oxide magnetic nanoparticles (MNs) coupled with FA enabled double targeted DOX delivery via a magnetic field, plus ligand-receptor interactions

• Increased cytotoxicity toward human glioblastoma (U87) cells  
• Internalized by U87 cells with consequent intracellular DOX release and transport into the nucleus, whereas the nanoparticles remained in the cytoplasm

---

**DOX-FA-PEG-SWCNTs** • Extremely high loading efficiency (149.3±4.1%) [98]

---

	DOX loaded onto the surface of SWCNTs, previously coated by FA-terminated polyethylene glycol (FA-PEG) via adsorption	<ul style="list-style-type: none"> <li>• Negligible cytotoxicity against normal (3T3) cells, whereas selectively entered HeLa cells via clathrin-mediated endocytosis, where DOX was released, subsequently entered the nucleus, thus causing cell death</li> </ul>	
	<b>DOX loaded anti-CD105 conjugated magnetic SWCNTs</b>	<ul style="list-style-type: none"> <li>• Improved targeting towards lung metastatic sites in a breast cancer animal model</li> <li>• Potential in cancer treatment efficiency at early, plus late phases of cancer progression</li> </ul>	[99]
	<b>DOX-DEX-fMWCNTs</b> DOX loaded onto dexamethasone (DEX) conjugated fMWCNTs	<ul style="list-style-type: none"> <li>• High loading efficiency (92.6±0.5%)</li> <li>• Low hemolyticity</li> <li>• Higher cytotoxicity against A549 cells</li> </ul>	[100]
	<b>Nanocomplex DOX-PEI-B-MWCNTs-siRNA</b> Polyethyleneimine (PEI) covalently coupled with betaine (PEI-B) and oMWCNTs and combined with DOX and survivin siRNA	<ul style="list-style-type: none"> <li>• Able to co-deliver DOX and siRNA into A549 cells, leading to the increase of the apoptotic index</li> <li>• Able to reduce the tumor volume in nude mice with A549 tumor cells without causing any damages to normal tissues</li> </ul>	[101]
<b>Etoposide (VP-16)</b>	<b>PEG-grafted MWCNTs (PEG-oMWCNTs) hybrid nanosystem</b> Carrier of the lung cancer drug VP-16 and Bcl-2 phosphorothioate antisense deoxyoligonucleotides	<ul style="list-style-type: none"> <li>• Higher cytostatic efficacy</li> <li>• Enhancement of the apoptotic cells against the small cell (SCLC; DMS53) and non-small cell lung cancer (NSCLC; NCIH2135) cell lines</li> </ul>	[102]

<b>Gemcitabine (GEM)</b>	<b>GEM-SWCNTs'</b> ; <b>GEM-PEG-SWCNTs"</b> GEM-SWCNTs and GEM-PEG-SWCNTs via carboxylation, acylation, amination, and PEGylation of pristine SWCNTs followed by gemcitabine (GEM) coupling	<ul style="list-style-type: none"> <li>GEM loading capacity of 43.14% (w/w)' and 37.32%"</li> <li>More cytotoxic against A549 and human pancreatic carcinoma (MIA PaCa-2) cell lines</li> <li>Superior efficacy in tumor growth suppression in B6 nude mice"</li> </ul>	[103]
<b>Methotrexate (MTX)</b>	<b>MTX-FA-AF-fMWCNTs</b> Theranostic prodrug, based on fMWCNTs co-tethered with MTX, a tumor targeting module (folic acid (FA)), a fluorochrome (Alexa-fluor (AF488/647)), and a radionuclide (Technetium-99m (99mTc))	<ul style="list-style-type: none"> <li>Selectively internalized by folate receptor (FR) positive A549 and MCF-7 cancer cells via FR-mediated endocytosis, consequently presenting superior anticancer activity</li> <li>The tumor-specific accumulation of MTX-FA-AF-fMWCNTs in Ehrlich Ascites tumor-bearing mice was nearly 19 and 8.6-fold superior to free MTX and MWCNTs without FA, respectively.</li> <li>MTX-FA-AF-fMWCNTs displayed superior tumor growth arrest while not showing any hepatotoxicity, cardiotoxicity, and nephrotoxicity in mice</li> </ul>	[104]
	<b>MTX-CHI-MWCNT nanohybrid</b>	<ul style="list-style-type: none"> <li>Negligible toxicity against healthy (MRC-5) cells</li> <li>Selective and pH-responsive MTX delivery to human lung cancer (H1299) cells</li> </ul>	[105]
<b>Paclitaxel (PTX)</b>	<b>PTX-fSWCNT/graphene oxide flakes</b>	<ul style="list-style-type: none"> <li>Superior cell death against NCI-H460 cells and mitogen associated protein kinase activation</li> </ul>	[106]

	<p><b>PTX-PCA-MWCNTs</b></p> <p>MWCNTs initially functionalized with hyperbranched poly citric acid (PCA), whose carboxyl functional groups were afterward coupled with PTX</p>	<ul style="list-style-type: none"> <li>• Drug encapsulation efficiency: 38% (w/w)</li> <li>• pH-responsive PTX release into tumor tissues and cells</li> <li>• Negligible toxicity against A549 and ovary cancer (SKOV3) cells</li> <li>• Higher cytotoxicity than free PTX over an inferior incubation time, indicating enhanced cell penetration</li> </ul>	[107]
	<p><b>PTX-PEG-SWCNT<sup>†</sup>;</b></p> <p><b>PTX-PEG-MWCNT<sup>‡</sup></b></p> <p>PTX physically loaded via immersion of PEG-SWCNT, plus PEG-MWCNT</p>	<ul style="list-style-type: none"> <li>• Loading capability: 26% (w/w)<sup>†</sup> and 36% (w/w)<sup>‡</sup></li> <li>• Sustainable PTX release in buffer solution</li> <li>• Superior efficacy against HeLa and MCF-7 cells</li> </ul>	[108]
	<p><b>PTX-SWCNTs</b></p> <p>Co-exposure of SWCNTs and PTX</p>	<ul style="list-style-type: none"> <li>• Increased cell death and apoptosis induction of human ovarian cancer (OVCAR3) cells</li> </ul>	[109]
	<p><b>PTX/HA-CHI-SWCNTs</b></p> <p>Chitosan non-covalently linked to SWCNTs, combined with HA connected to the outer CHI layer, later attached to PTX</p>	<ul style="list-style-type: none"> <li>• Negligible toxicity toward normal fibroblast cells, besides enhanced toxicity and apoptosis induction to A549 cells</li> </ul>	[110]
<b>Pt(IV)</b>	<p><b>Pt(IV)-fSWCNT conjugate</b></p>	<ul style="list-style-type: none"> <li>• Successfully delivered a lethal dosage of cis-[Pt(NH<sub>3</sub>)<sub>2</sub>Cl<sub>2</sub>] upon intracellular reduction</li> <li>• Substantially enhanced cytotoxicity profile against testicular carcinoma (NTera-2) cells</li> </ul>	[111]

		<b>Pt(IV)-fMWCNTs</b> Properly load an inert Pt(IV) complex into fMWCNTs	<ul style="list-style-type: none"> <li>Administration in mice considerably augmented the Pt content in certain tissues (especially lung, liver, and spleen) while not causing inflammatory reaction or necrosis [112]</li> </ul>
Antihypertensive drugs	<b>Candesartan (CD)</b>	<b>iRGD-PEI-MWCNT-SS-CD/pAT2 complexes</b> Tumor-homing peptide (iRGD) attached to PEI connected to MWCNT skeleton, combined with CD linked via cystamine (SS) to the MWCNT, all of which assembled by plasmid AT2 (pAT2)	<ul style="list-style-type: none"> <li>Significant neovascularization and tumor growth suppression in A549 xenograft nude mice [113]</li> </ul>
	<b>Glucocorticoid</b>	<b>VA-fMWCNTs</b> Vertically aligned (VA)-MWCNTs functionalized and PEGylated, before the loading of glucocorticoid	<ul style="list-style-type: none"> <li>Enhancement of drug release, displaying 55%, 65%, and 95% release at pH 7.4, 6.5, and 5.5, respectively [114]</li> <li>Shallow cytotoxicity effect in PC-12 cells</li> </ul>
Corticosteroids			

Drug delivery systems: 'GEM-SWCNTs; " GEM-PEG-SWCNTs; † PTX-PEG-SWCNT; ‡ PTX-PEG-MWCNT.

### 2.3.2. Genes and nucleic acids

Several DDS containing genes and nucleic acids, such as oligodeoxynucleotides, oligonucleotides, plasmid DNA (pDNA), aptamers, and small-interfering RNA (siRNA) linked to CNTs were studied aiming their intracellular transporting and controlled release [27, 115–118]. In this field, Jia et al. [115] developed a double functionalization of MWCNT delivery method comprising therapeutic gene antisense oligodeoxynucleotides and fluorescent labeling probes mercaptoacetic acid-capped CdTe quantum dots, through electrostatically layer-by-layer assembling. These fMWCNTs enabled a successful intracellular transporting, cell nucleus localization, delivery efficiency, and anticancer activity against HeLa cells, revealing the potential for biological delivery and gene therapy [115]. Polyamidoamine dendrimer modified MWCNTs (dMWCNTs) coupled with the FI-labeled antisense c-myc oligonucleotides displayed high transfection efficiencies and successfully hindered cell growth in time- and dose-dependent ways in MCF-7, MDA-MB-435 and HepG2 cells, showing its potential for cancer therapy and molecular imaging [117].

A novel pDNA-fSWCNTs-based gene delivery vector method was developed [27] based on fSWCNTs complexed with pDNA. These were prepared via electrostatic interactions, which could bind and enter HeLa cells, while enhancing DNA uptake and gene expression in Chinese hamster ovary (CHO) cells [27]. Ammonium-functionalized SWCNTs with pDNA (pDNA-NH<sub>3</sub><sup>+</sup>-SWCNT) complexes, as well as established lysine (Lys)-functionalized SWCNTs (pDNA-NH<sub>3</sub><sup>+</sup>-Lys-SWCNT) and NH<sub>3</sub><sup>+</sup>-functionalized MWCNTs with pDNA (pDNA-NH<sub>3</sub><sup>+</sup>-MWCNT) complexes, were able to transfect A549 cells with distinct efficiency levels, displaying their potential as a successful gene delivery vector method [119].

EpCAM RNA aptamer-piperazine-PEI-SWCNT based on RNA aptamer against epithelial cell adhesion molecule (EpCAM) physically attached to SWCNT conjugated to piperazine-PEI derivative was reported to specifically induce apoptosis in MCF-7 cells, besides leading to BCL9I (related to breast and colorectal cancers) protein level decrease, further showing its targeted silencing activity [120]. In a similar work, anti MUC1-aptamer-cMWCNT hybrid based on anti MUC1 (membrane-associated glycoform overexpressed on a wide range of epithelial cancer cells)-aptamers covalently grafted onto cMWCNTs were able to translocate into MCF-7 cytoplasm via a receptor-independent manner [116].

Regarding DDS with siRNA, Varkouhi et al. [121] showed the potential of MWCNTs covalently functionalized with PEI (PEI-MWCNTs) and MWCNTs non-covalently functionalized with cationic pyridinium (Pyrr-MWCNTs) complexed with anti-luciferase siRNA in displaying a silencing activity between 10 and 30% and cytotoxicity between 10 and 60%. These results were similar



to the controls (PEI and reference transfectants (Lipofectamine 2000, pDMAEMA)) [121]. Polo-Like Kinase1 (PLK1) was confirmed as a cancer gene therapy target through the association between PLK1 siRNA and fMWCNTs as delivery vectors [118]. This association allowed the enhancement of siRNA retention in a solid tumor and increased tumor cellular uptake *in vivo*, which subsequently prolonged animal survival of human lung carcinoma (Calu6) xenografts bearing mice [118]. Furthermore, siTOX-NH<sub>3</sub><sup>+</sup>-MWCNT complexes based on proprietary cytotoxic siRNA sequence (siTOX) complexed with NH<sub>3</sub><sup>+</sup>-functionalized MWCNTs (NH<sub>3</sub><sup>+</sup>-MWCNT) were able to delay tumor growth [122]. siTOX-NH<sub>3</sub><sup>+</sup>-MWCNT complexes enhanced the survival of xenograft-bearing animals following its intratumoral administration [122]. Al-Jamal et al. [123] revealed the perilesional stereotactic administration of Caspase-3 siRNA (siCas 3) delivered by NH<sub>3</sub><sup>+</sup>-MWCNT enabled neuroprotection, following focal ischemic damage caused by Endothelin-1 in the motor cortex of both mice and rats, leading to functional recovery as displayed by the “skilled reaching” test in living rats. In the same line, Ladeira et al. [124] showed that siRNA-fSWCNTs could be applied as delivery systems to different cell types, such as non-metastatic human hepatocellular carcinoma (SKHep1), cardiomyocytes, and rat dorsal root ganglion (DRG) neuron cells, while displaying a successful target gene silencing with high specificity and reduced toxicity. Kam et al. [125] also developed siRNA-SS-PL-PEG-SWCNTs based on the strong binding of phospholipid molecules with PEG (PL-PEG) to SWCNTs, followed by the cleavable disulfide linkage between PL-PEG-SWCNTs and siRNA, which attained high siRNA efficiency delivery in HeLa cells. Chen et al. [126] reported SWCNTs functionalization with DSPE-PEG-Amine allowed siRNA binding via disulfide bonds, reaching a siRNA loading efficiency of 83.55%. In fact, siRNA specifically targeting the oncogene Murine Double Minute Clone 2 (MDM2 siRNA) coupled with fSWCNTs managed to enter breast cancer (B-Cap-37) cells, with MDM2 siRNA being subsequently released due to disulfide bonds digestion by intracellular enzymes, thus inhibiting cell proliferation and promoting apoptosis [126]. Bartholomeusz et al. [127] demonstrated that siRNA-SWCNTs complexes with hypoxia-inducible factor 1 alpha (HIF-1α)-targeted siRNA (HIF-1α siRNA) were able to inhibit cellular HIF-1α activity in a pancreatic cell line with HIF-1α/ luciferase reporter (MiaPaCa2-HRE) cells. HIF-1α siRNA-SWCNTs complexes intratumorally administrated in mice bearing MiaPaCa-2/HRE tumors led to HIF-1α activity inhibition, showing its potential in human cancer cases with resistance to therapy [127].

### **2.3.3. Proteins, peptides, and ligands**

Numerous proteins, peptides, and ligands, namely BSA, trypsin, pepsin, lysozyme, ferritin, fibrinogen, papain, hemoglobin, recombinant ricin A chain protein (RTA), Streptavidin (SA),

asparagine-glycine-arginine (NGR), and tumor necrosis factor-related apoptosis-inducing ligand (TRAIL), linked to CNTs were applied in DDS, envisioning their uptake by cells and increased cytotoxicity [128–131]. Parra et al. [132] developed AZc6-BSA-CNTs conjugates based on azoxystrobin (AZ), a strobilurin fungicide, and a derivative bearing a carboxylated spacer arm (hapten AZc6) covalently linked to BSA, afterward covalently associated to fCNTs with distinct shapes and sizes. Immunization of New Zealand rabbits and BALB/c mice with AZc6-BSA-CNTs conjugates triggered significant IgG responses with and without an adjuvant, thus showing CNTs' self-adjuvant ability. From all tested conditions, the best antibody response was produced by short and thick AZc6-BSA-CNTs conjugates. In fact, low dosages (0.05 µg) of AZc6-BSA-CNTs conjugates had strong anti-AZ immune responses in rabbits [132]. CHI NPs-MWCNT hybrids were synthesized via an ionotropic gelation method enabled high (76.8%) BSA immobilization efficiency and biocompatibility with HeLa cells since cell viability is 81%, following 24 h incubation with 100 µg mL<sup>-1</sup> [133]. SWCNTs were functionalized with cationic-designed amphiphilic polypeptides and subsequent protein binding, e.g., BSA, trypsin, pepsin, lysozyme, ferritin, fibrinogen, papain, and hemoglobin or DNA via a bilayer approach [128]. Their delivery efficiency into HeLa cells was affected by the complexes charge, showing its potential as delivery systems [128]. This model that predicts natural proteins' adsorption onto SWCNT, based on its structure and composition, was reported for the first time [128]. RTA-MWCNTs conjugates induced target destruction of tumor cells, particularly HeLa cells, whose cell mortality reached around 75% [134]. Actually, HER2-RTA-MWCNTs obtained by attaching HER2 onto RTA-MWCNTs conjugates led to selective destruction of HER2 overexpressing breast cancer cells [134]. SA-biotin-SWCNTs conjugates based on fluoresceinated SA, a protein with anticancer applications complexed with the biotin-SWCNTs transporter, were uptake through endocytosis into human promyelocytic leukemia (HL60) and human T (Jurkat) cells, displaying dose-dependent cytotoxicity [129].

Concerning the use of peptides in DDS, TAM-NGR-SWCNTs conjugates based on SWCNTs functionalized with NGR, subsequently loaded with tamoxifen (TAM), an anticancer drug, attained high cellular uptake, cytotoxicity, and cell apoptosis *in vitro* due to its receptor-mediated tumor-targeting potential [130]. In another work with SWCNTs, TRAIL-based SWCNTs nanovectors shown to be highly efficient in triggering cancer cell killing, increasing apoptosis *in vitro* due to their capacity to enhance caspase-8 activation [131].

## 2.4. Carbon Nanotubes in Targeted Therapies

CNTs have intrinsic physical features, which allied with suitable functionalization, enable their use in photothermal therapy (PTT), photodynamic therapy (PDT), and the combination of both [30, 135, 136].

### 2.4.1. Photothermal therapy

PTT is a noninvasive, harmless, and efficient therapeutic technology that enables tumor cells' death via locally heated tumor tissues by near-infrared region absorption [30, 137, 138]. Therefore, CNTs have been applied in PTT due to their ability to absorb light in the near-infrared region and successfully transform absorbed energy into released heat [30, 139–142].

Regarding PTTs using SWCNTs, Shao et al. [143] prepared anti-IGF1-anti-HER2-SWCNTs hybrids based on SWCNTs functionalized with insulin-like growth factor 1 receptor (IGF1R), as well as human endothelial receptor 2 (HER2) specific antibodies. These hybrids targeted their corresponding receptors in breast cancer cells, allowing SWCNTs' internalization, and by a near-infrared region they were able to destroy all treated cells, whereas non-specific-antibody-SWCNT hybrids only killed 20% of the cells [143]. Specific binding of SWCNTs dispersions were prepared with human anti-CD22 antibodies, followed by exposure to near-infrared region leading to highly specific ablation of human Burkitt's lymphoma cells *in vitro* [31]. FA-CoMoCAT® SWCNTs conjugates exhibited an effective increased photothermal destruction on tumor cells while sparing non-targeted normal cells in both *in vitro* and *in vivo* experiments [144]. Xiao et al. [145] demonstrated the selective photothermal ablation after near-infrared region irradiation of HER2 immunoglobulin Y (IgY)-SWCNT complexes based on the covalent conjugation between cSWCNTs and anti-HER2 chicken IgY antibodies, specifically targeted HER2-expressing SK-BR-3 cells. HER2 IgY-SWCNT complexes allowed the detection, and selective photothermal ablation of receptor-positive breast cancer cells without cells' internalization [145]. A combination between intratumoral injection of PEG-SWCNTs and near-infrared irradiation allowed the complete destruction of solid malignant tumors devoid of side effects or tumor recurrence over 6 months [146]. The majority of injected SWCNTs were excreted from mice bodies in 2 months via biliary or urinary pathways [146]. The combination between the injection of SWCNTs and 10 minutes of near-infrared region irradiation eradicated squamous cell carcinomas, and SWCNTs remained exclusively in the tumor even 3 months following injection [147]. Mitochondria targeting SWCNTs, after near-infrared region irradiation, were able to destroy the targeted mitochondria selectively, thus inducing apoptosis, and tumor growth suppression was achieved in a breast cancer model [148]. Zhou et al. [149] displayed glycosylated CHI-SWCNTs, after near-

infrared region irradiation, induced photothermal death of mouse mammary tumor (EMT6) cells *in vitro* and *in vivo*, enabling complete tumor regression, as well as long-term survival in several cases. NGR-siRNA-PEI-SWCNTs, based on the functionalization of SWCNTs with PEI, were further conjugated with the tumor-targeting NGR peptide and loaded with hTERT siRNA, which were enabled *in vitro* apoptosis induction in PC-3 cells, besides high antitumor activity *in vivo* [150]. The combination of DOX-loaded SWCNTs (DOX-SWCNTs) and near-infrared region irradiation enabled an efficient MDA-MB-231 cell death via mitochondrial disruption, as well as ROS generation [151]. The combination of water-soluble fSWCNTs, followed by 2 minutes of radiofrequency field treatment, led to the destruction of almost all hepatocellular cancer (HepG2, Hep3B), plus pancreatic adenocarcinoma (Panc-1) cells *in vitro* [140]. In fact, fSWCNTs injection into hepatic (VX2) tumors in rabbits, immediately followed by radiofrequency field, led to total necrosis of all treated tumors after 48 hours [140].

Concerning PTTs using MWCNTs, Torti et al. [152] reported that nitrogen-doped MWCNTs (CNx-MWCNTs) led to the destruction of kidney cancer cells following near-infrared region irradiation. Anti-GD2 monoclonal antibody conjugated to MWCNTs highly internalized by neuroblastoma (stNB-V1) cells, through GD2-mediated endocytosis and irradiated with near-infrared region treatment, led to necrosis of all stNB-V1 cells, whereas all nontargeted normal cells remained viable [153]. Complete photothermal kidney tumor ablation was achieved using MWCNTs; 80% of mice were alive, plus tumor-free, following 3 months treatment with a proper amount of MWCNTs [154]. Intratumoral injection of DNA-encased MWCNTs, followed by near-infrared region irradiation, enabled a total eradication of PC3 xenograft tumors in all treated mice [142]. In fact, DNA-encasement allowed a 3-fold decrease in the concentration of MWCNTs needed for a 10°C temperature rise in bulk solution temperature [142]. Also, Burlaka et al. [155] demonstrated MWCNTs led to the destruction of 95.2% of Erlich ascitic carcinoma (EAC) cells, following 1.5 min of near-infrared region irradiation [155] and the conjugation between P-Glycoprotein-targeted MWCNTs and near-infrared region irradiation caused high cytotoxicity in multidrug resistance cancer cells [156].

#### **2.4.2. Photodynamic therapy**

PDT is a local noninvasive cancer treatment, which comprises the administration of a nontoxic photosensitizer, afterward activated by a suitable harmless light source [135, 157, 158]. The photosensitizer generates highly reactive singlet oxygen ( $^1\text{O}_2$ ) via light energy transfer to the tissue oxygen, an aggressive chemical species that mediates cellular toxicity leading to cell damage and eventually cell death [135, 157, 158]. For instance, Zhu et al. [135] reported, as a

proof of concept for PDT, that single-stranded DNA aptamer (ssDNA AP)-photosensitizer-SWCNTs based on the attachment of ssDNA AP and photosensitizer on SWCNTs, allowed controllable  $^1\text{O}_2$  generation via target binding [159]. The noncovalent interaction between pyrenyl-functionalized distyryl-dodipy sensitizer and SWCNTs generated  $^1\text{O}_2$  after irradiation at 660 nm [159]. Additionally, Xiao et al. [160] prepared CHI-Ce6-SWCNTs based on the noncovalent attachment of the photosensitizer chlorin e6 (Ce6) and SWCNTs, afterward wrapped by CHI to improve biocompatibility and aqueous solubility, and demonstrated their low dark toxicity and efficient PDT efficacy towards HeLa cells. PEI-SWCNTs based on SWCNTs covalent functionalized with PEI revealed a strong photodynamic *in vitro* and *in vivo* effect on mice melanoma B16F10 cells and tumor-bearing mice, showing their potential for cancer PDT [161].

#### **2.4.3. Combination of photothermal and photodynamic therapies**

The combination of PTD and PDT has received significant interest in cancer treatment due to its potential synergistic effect [162]. Shi et al. [163] reported the HMME-HA-SWCNTs based on HA-derivatized SWCNTs, followed by the adsorption of hematoporphyrin monomethyl ether (HMME), enabled *in vivo* melanoma B16F10-bearing mice growth inhibition via a synergistic effect of local specific PDT, as well as external near-infrared region PTT. Ru-SWCNTs were loaded with two-photon luminescent Ru(II) complexes onto SWCNTs [162]. After irradiation at 808 nm, Ru(II) complexes are released, producing  $^1\text{O}_2$  upon two-photon laser irradiation. High anticancer efficacies were obtained in HeLa cancer cells, in addition to multicellular tumor spheroids, as well as *in vivo* tumor ablation [162]. mTHPC-MWCNTs performance comprising the photosensitizer m-tetrahydroxyphenylchlorin (mTHPC) and MWCNTs depend on the irradiation conditions, leading to the synergistic apoptosis of the whole SKOV3 cell population [136].

### **3. Toxicity of carbon nanotubes**

The toxicity of CNTs is a subject of some controversy in the literature. A significant amount of works dealing with this issue can be found, particularly to address whether or not CNTs are potentially harmful to organisms and if they have potential application in biomedicine. CNTs toxicity was determined by both *in vivo* and *in vitro* tests. *In vivo* toxicity analysis of CNTs is commonly performed by evaluating specific organs and biodistribution in mice and rats, while *in vitro* toxicity tests use animal cell lines and microbes (bacteria, yeast). In particular, the CNTs toxicity was evaluated through cell proliferation/viability tests, apoptosis detection, ROS generation, and superoxide dismutase quantification [164, 165].

Injection, ingestion, and inhalation are the three possible ways for CNTs to enter the human body. Once inside the organism, CNTs can interact with cells in different ways or even cross them, reaching the bloodstream and spread to numerous parts of the body [166]. The main effects behind CNTs toxicity are oxidative stress, inflammatory responses, DNA damage or mutation, malignant transformation, interstitial fibrosis and granuloma [19, 167–169], thus affecting several organs, like liver and kidney [170], and pulmonary [171], reproductive [172, 173] and nervous [174] systems. For instance, Czarny et al. [175] reported a high CNTs bio-persistence, remaining in the organism for 12 months. CNTs organ biodistribution and bio-persistence depend on diverse physicochemical properties, such as CNTs degree and type of surface functionalization, dispersibility, length, and metal impurities [176].

Several authors have been reporting the reduction of CNTs toxicity by functionalization. For example, Ali-Boucetta et al. [176] showed that the higher the functionalization degree of the CNT surface, the less the accumulation in reticuloendothelial system (RES) organs and the higher the CNTs urinary excretion. Jain et al. [177] also observed a rapid elimination from the organism of highly oxidized MWCNTs through renal excretion without causing nephrotoxicity. In contrast, pristine and less oxidized MWCNTs revealed greater retention in RES organs. Another work showed reduced toxic effects on human umbilical vein endothelial cells when exposed to hydroxylated or carboxylated MWCNTs [178]. The conjugation with biocompatible materials, like PEG, has also proved to reduce CNTs toxicity [179]. No toxic effects of PEGylated SWCNTs was reported after 3 months of *in vivo* tests in mice [57]. Conversely, De Marchi et al. [180] demonstrated that carboxylated MWCNTs induced toxicity in suspension-feeding polychaetes *Ficopomatus. enigmaticus*, negatively affecting their biochemical and physiological status.

The degree of dispersibility is also an important parameter to take into account regarding CNTs toxicity. More dispersed CNTs cause less toxic effects since agglomerated particles tend to accumulate more quickly in vital organs, leading to inflammatory responses or possible cell-damaging [181]. Yang et al. [182] detected long-term cytotoxic effects promoted by the aggregation of SWCNTs and their accumulation in the lungs of mice. However, the toxicity of the dispersant and its dosage must be taken into account. An increase in the SWCNTs toxicity was demonstrated with the solubilizing agent toxicity [183]. Additionally, the SWCNTs dispersion in water by sodium dodecyl sulfate (SDS) was studied, revealing an inhibition of the growth of kidney epithelial cells (NRK-52E) in rats at low concentrations and an increase in the number of cells in the apoptotic sub-G(1) phase with increasing dispersant concentration [184].

The particle length affects the CNT toxicity essentially regarding their cellular internalization. Raffa et al. [185] demonstrated that the smaller the CNTs, the easier the penetration to the cell membrane. In turn, Murphy et al. [186] studied the direct instillation of long and short CNTs into

the pleural cavity. They observed the clearance of short CNTs, whereas the retention of the long ones caused acute inflammation on the parietal pleura. It has to be noted that during the functionalization process, most of the CNTs are broken into smaller particles, making it difficult to confirm which parameter most influences their toxicity, whether functionalization or length. Nevertheless, more recently, in a study about the influence of MWCNTs diameters on the toxicity to human endothelial cells, a decrease in cytotoxicity with the increase of MWCNTs diameters was reported [187]. The smallest MWCNTs induced cytokine release, THP-1 monocyte adhesion, and ROS generation. Also, Yamashita et al. [188] revealed that the CNTs toxicity depends not only on their length but also on their thickness. These authors evaluated SWCNTs and different sized MWCNTs, detecting DNA damage and severe inflammatory effects caused by long and thick MWCNTs, but not by short and thin ones or by SWCNTs.

Another important factor in CNTs toxicity is the amount and type of metal impurities introduced during the synthesis step. It was observed that commercial non-purified CNTs caused oxidative stress in cells, while acid-purified ones, with almost no metal content, revealed slight or no cytotoxic effects [189]. Inhibition of cell proliferation by MWCNTs impurities was also reported [190]. Nevertheless, Cheng et al. [191] did not detect differences in human macrophage cell death after exposure to non-purified or heat-purified MWCNTs. In fact, the CNTs impurities contribution toward toxicity should consider the impurities dosage, the administration method, and the method used to detect that contribution [19].

The potential CNTs toxicity is still a topic of debate, which is even more exacerbated due to the CNTs panoply, i.e. with diverse morphologies and purities, as well as several biological media with different concentrations (*in vitro*, *in vivo*, primary cells, cancer cell lines, several animal models) and numerous techniques of dispersion, exposure and characterization of CNTs. Moreover, the CNTs exposure to real circumstances is difficult to measure, and the dosages used are far from reality. Further toxicity studies are crucially needed to identify the CNTs safety limit value and to elucidate their toxicological mechanism.

#### **4. Conclusions and future perspectives**

CNTs are promising materials and have been extensively investigated for biomedical applications due to their unique structure and excellent properties, such as strong loading capacity, biocompatibility, high surface area, high strength, and enhanced chemical and thermal stability. CNTs have been applied in the pharmacy and medicine fields, namely in diagnostics and diseases monitoring, due to their high conductivity; tissue engineering; drug and gene delivery to cells or organs owing to their large surface area; and targeted therapies, on account of their nanoscale diameters that enable them to penetrate the cell membrane. However, their

use in biomedical applications raises some questions in what concerns safety and potential toxicity. However, up to date it is clear that CNTs toxicity depends on their structure, morphology and surface functional groups. To decrease their toxicity and improve biocompatibility, surface functionalization of CNTs has been widely investigated.

Although numerous reports described CNTs for biosensing, bioimaging, drug delivery, and therapy, additional investigations are still needed to spread the CNTs use in the biomedical field in the future and under safe conditions. In specific, more efforts on the evolution of the *in vitro* and *in vivo* CNTs toxicity are required to clarify their long-term effects so that their application could become more frequent and widespread.

### Acknowledgments

This work was developed within the scope of the project CICECO-Aveiro Institute of Materials, UIDB/50011/2020 & UIDP/50011/2020, financed by national funds through the Portuguese Foundation for Science and Technology/MCTES. This work was financially supported by Base Funding - UIDB/EQU/50020/2020 of the Associate Laboratory LSRE-LCM - funded by national funds through FCT/MCTES (PIDDAC), and POCI-01-0145-FEDER-031268 - funded by FEDER, through COMPETE2020 - Programa Operacional Competitividade e Internacionalização (POCI), and by national funds (OE), through FCT/MCTES. João C. F. Nunes acknowledges SPQ and FCT for the PhD fellowship (SFRH/BD/150671/2020). Raquel O. Cristóvão acknowledges FCT funding under DL57/2016 Transitory Norm Programme. Ana P.M. Tavares acknowledges the FCT Investigator Programme and Exploratory Project (IF/01634/2015) with financing from the European Social Fund and the Human Potential Operational Programme.

### 5. References

1. Tejendra Kumar G, Pattabhi Ramaiah B, Sivakumar Reddy C, Sudhir Sastry YB, Marco P, Stephane PB (2019) Advances in Carbon Based Nanomaterials for Bio-Medical Applications. *Curr Med Chem* 26:6851–6877 .  
<https://doi.org/http://dx.doi.org/10.2174/0929867326666181126113605>
2. Hong G, Diao S, Antaris AL, Dai H (2015) Carbon Nanomaterials for Biological Imaging and Nanomedicinal Therapy. *Chem Rev* 115:10816–10906 .  
<https://doi.org/10.1021/acs.chemrev.5b00008>
3. Rajakumar G, Zhang X-H, Gomathi T, Wang S-F, Ansari MA, Mydhili G, Nirmala G, Alzohairy MA, Chung I-M (2020) Current Use of Carbon-Based Materials for Biomedical Applications—A Prospective and Review. *Processes* 8:355
4. Maiti D, Tong X, Mou X, Yang K (2019) Carbon-Based Nanomaterials for Biomedical Applications: A Recent Study. *Front Pharmacol* 9:1401 .  
<https://doi.org/10.3389/fphar.2018.01401>
5. Bhattacharya K, Mukherjee SP, Gallud A, Burkert SC, Bistarelli S, Bellucci S, Bottini M, Star A, Fadeel B (2016) Biological interactions of carbon-based nanomaterials: From coronation to degradation. *Nanomedicine Nanotechnology, Biol Med* 12:333–351 .  
<https://doi.org/https://doi.org/10.1016/j.nano.2015.11.011>
6. Iijima S (1991) Helical microtubules of graphitic carbon. *Nature* 354:56–58 .  
<https://doi.org/10.1038/354056a0>
7. Balasubramanian K, Burghard M (2005) Chemically functionalized carbon nanotubes. *Small* 1:180–192 . <https://doi.org/10.1002/sml.200400118>
8. Dettlaff A, Sawczak M, Klugmann-Radziemska E, Czyłkowski D, Miotk R, Wilamowska-



- Zawłocka M (2017) High-performance method of carbon nanotubes modification by microwave plasma for thin composite films preparation. *RSC Adv* 7:31940–31949 . <https://doi.org/10.1039/C7RA04707J>
9. Dong X, Wei C, Liang J, Liu T, Kong D, Lv F (2017) Thermosensitive hydrogel loaded with chitosan-carbon nanotubes for near infrared light triggered drug delivery. *Colloids Surf B Biointerfaces* 154:253–262 . <https://doi.org/10.1016/j.colsurfb.2017.03.036>
  10. Verma SK, Modi A, Bellare J (2019) Polyethersulfone-carbon nanotubes composite hollow fiber membranes with improved biocompatibility for bioartificial liver. *Colloids Surf B Biointerfaces* 181:890–895 . <https://doi.org/10.1016/j.colsurfb.2019.06.051>
  11. Raphey VR, Henna TK, Nivitha KP, Mufeedha P, Sabu C, Pramod K (2019) Advanced biomedical applications of carbon nanotube. *Mater Sci Eng C* 100:616–630 . <https://doi.org/https://doi.org/10.1016/j.msec.2019.03.043>
  12. Tasis D, Tagmatarchis N, Bianco A, Prato M (2006) Chemistry of Carbon Nanotubes. *Chem Rev* 106:1105–1136 . <https://doi.org/10.1021/cr050569o>
  13. Wu H-C, Chang X, Liu L, Zhao F, Zhao Y (2010) Chemistry of carbon nanotubes in biomedical applications. *J Mater Chem* 20:1036–1052 . <https://doi.org/10.1039/B911099M>
  14. Wang J (2005) Carbon-Nanotube Based Electrochemical Biosensors: A Review. *Electroanalysis* 17:7–14 . <https://doi.org/https://doi.org/10.1002/elan.200403113>
  15. He H, Pham-Huy LA, Dramou P, Xiao D, Zuo P, Pham-Huy C (2013) Carbon Nanotubes: Applications in Pharmacy and Medicine. *Biomed Res Int* 2013:578290 . <https://doi.org/10.1155/2013/578290>
  16. Anzar N, Hasan R, Tyagi M, Yadav N, Narang J (2020) Carbon nanotube - A review on Synthesis, Properties and plethora of applications in the field of biomedical science. *Sensors Int* 1:100003 . <https://doi.org/https://doi.org/10.1016/j.sintl.2020.100003>
  17. Monthieux M, Serp P, Flahaut E, Razafinimanana M, Laurent C, Peigney A, Bacsa W, Broto J-M (2010) Introduction to Carbon Nanotubes. In: Bhushan B (ed) *Springer Handbook of Nanotechnology*. Springer Berlin Heidelberg, Berlin, Heidelberg, pp 47–118
  18. Singh BGP, Rao CH, Pispati V, Pathipati H, Muthy N, Prassana SR V, Rathode BG (2012) Carbon nanotubes. A novel drug delivery system. *Int J Res Pharm Chem* 2:523–532
  19. Usui Y, Haniu H, Tsuruoka S, Saito N (2012) Carbon Nanotubes Innovate on Medical Technology. *Med Chem (Los Angeles)* 02: . <https://doi.org/10.4172/2161-0444.1000105>
  20. Alshehri R, Ilyas AM, Hasan A, Arnaout A, Ahmed F, Memic A (2016) Carbon Nanotubes in Biomedical Applications: Factors, Mechanisms, and Remedies of Toxicity. *J Med Chem* 59:8149–8167 . <https://doi.org/10.1021/acs.jmedchem.5b01770>
  21. Elhissi AMA, Ahmed W, Hassan IU, Dhanak VR, D’Emanuele A (2012) Carbon Nanotubes in Cancer Therapy and Drug Delivery. *J Drug Deliv* 2012:837327 . <https://doi.org/10.1155/2012/837327>
  22. Yang N, Chen X, Ren T, Zhang P, Yang D (2015) Carbon nanotube based biosensors. *Sensors Actuators B Chem* 207:690–715 . <https://doi.org/https://doi.org/10.1016/j.snb.2014.10.040>
  23. Lefebvre J, Austing DG, Bond J, Finnie P (2006) Photoluminescence Imaging of Suspended Single-Walled Carbon Nanotubes. *Nano Lett* 6:1603–1608 . <https://doi.org/10.1021/nl060530e>
  24. Murakami Y, Einarsson E, Edamura T, Maruyama S (2005) Polarization dependent optical absorption properties of single-walled carbon nanotubes and methodology for the evaluation of their morphology. *Carbon N Y* 43:2664–2676 . <https://doi.org/https://doi.org/10.1016/j.carbon.2005.05.036>
  25. Dresselhaus MS, Dresselhaus G, Saito R, Jorio A (2005) Raman spectroscopy of carbon nanotubes. *Phys Rep* 409:47–99 . <https://doi.org/https://doi.org/10.1016/j.physrep.2004.10.006>

26. Yu M-F, Lourie O, Dyer MJ, Moloni K, Kelly TF, Ruoff RS (2000) Strength and Breaking Mechanism of Multiwalled Carbon Nanotubes Under Tensile Load. *Science* (80- ) 287:637 . <https://doi.org/10.1126/science.287.5453.637>
27. Pantarotto D, Singh R, McCarthy D, Erhardt M, Briand JP, Prato M, Kostarelos K, Bianco A (2004) Functionalized carbon nanotubes for plasmid DNA gene delivery. *Angew Chemie - Int Ed* 43:5242–5246 . <https://doi.org/10.1002/anie.200460437>
28. Pantarotto D, Partidos CD, Graff R, Hoebeke J, Briand J-P, Prato M, Bianco A (2003) Synthesis, Structural Characterization, and Immunological Properties of Carbon Nanotubes Functionalized with Peptides. *J Am Chem Soc* 125:6160–6164 . <https://doi.org/10.1021/ja034342r>
29. Zhang W, Zhang Z, Zhang Y (2011) The application of carbon nanotubes in target drug delivery systems for cancer therapies. *Nanoscale Res Lett* 6:555 . <https://doi.org/10.1186/1556-276x-6-555>
30. Kam NW, O’Connell M, Wisdom JA, Dai H (2005) Carbon nanotubes as multifunctional biological transporters and near-infrared agents for selective cancer cell destruction. *Proc Natl Acad Sci U S A* 102:11600–11605 . <https://doi.org/10.1073/pnas.0502680102>
31. Chakravarty P, Marches R, Zimmerman NS, Swafford ADE, Bajaj P, Musselman IH, Pantano P, Draper RK, Vitetta ES (2008) Thermal ablation of tumor cells with antibody-functionalized single-walled carbon nanotubes. *Proc Natl Acad Sci U S A* 105:8697–8702 . <https://doi.org/10.1073/pnas.0803557105>
32. Simon J, Flahaut E, Golzio M (2019) Overview of Carbon Nanotubes for Biomedical Applications. *Mater (Basel, Switzerland)* 12:624 . <https://doi.org/10.3390/ma12040624>
33. Yang W, Ratinac KR, Ringer SP, Thordarson P, Gooding JJ, Braet F (2010) Carbon Nanomaterials in Biosensors: Should You Use Nanotubes or Graphene? *Angew Chemie Int Ed* 49:2114–2138 . <https://doi.org/https://doi.org/10.1002/anie.200903463>
34. Punbusayakul N, Talapatra S, Ajayan PM, Surareungchai W (2013) Label-free as-grown double wall carbon nanotubes bundles for Salmonella typhimurium immunoassay. *Chem Cent J* 7:102 . <https://doi.org/10.1186/1752-153X-7-102>
35. Zhou J, Li H, Yang H, Cheng H, Lai G (2017) Immobilization of Glucose Oxidase on a Carbon Nanotubes/Dendrimer-Ferrocene Modified Electrode for Reagentless Glucose Biosensing. *J Nanosci Nanotechnol* 17:212–216 . <https://doi.org/10.1166/jnn.2017.12388>
36. Shrestha BK, Ahmad R, Mousa HM, Kim I-G, Kim JI, Neupane MP, Park CH, Kim CS (2016) High-performance glucose biosensor based on chitosan-glucose oxidase immobilized polypyrrole/Nafion/functionalized multi-walled carbon nanotubes bio-nanohybrid film. *J Colloid Interface Sci* 482:39–47 . <https://doi.org/https://doi.org/10.1016/j.jcis.2016.07.067>
37. Devasenathipathy R, Mani V, Chen S-M, Huang S-T, Huang T-T, Lin C-M, Hwa K-Y, Chen T-Y, Chen B-J (2015) Glucose biosensor based on glucose oxidase immobilized at gold nanoparticles decorated graphene-carbon nanotubes. *Enzyme Microb Technol* 78:40–45 . <https://doi.org/https://doi.org/10.1016/j.enzmictec.2015.06.006>
38. Zhang X, Xu Y, Ye B (2018) An efficient electrochemical glucose sensor based on porous nickel-based metal organic framework/carbon nanotubes composite (Ni-MOF/CNTs). *J Alloys Compd* 767:651–656 . <https://doi.org/https://doi.org/10.1016/j.jallcom.2018.07.175>
39. LI Y-W, CHEN Y, MA Y-H, SHI J-G, WANG Y-X, QI C-H, LI Q-S (2014) Recent Advances in the Dehydrogenase Biosensors Based on Carbon Nanotube Modified Electrodes. *Chinese J Anal Chem* 42:759–765 . [https://doi.org/https://doi.org/10.1016/S1872-2040\(13\)60733-1](https://doi.org/https://doi.org/10.1016/S1872-2040(13)60733-1)
40. Kafi AKM, Naqshabandi M, Yusoff MM, Crossley MJ (2018) Improved peroxide biosensor based on Horseradish Peroxidase/Carbon Nanotube on a thiol-modified gold electrode. *Enzyme Microb Technol* 113:67–74 .

- <https://doi.org/https://doi.org/10.1016/j.enzmictec.2017.11.006>
41. He P, Dai L (2004) Aligned carbon nanotube–DNA electrochemical sensors. *Chem Commun* 348–349 . <https://doi.org/10.1039/B313030B>
  42. Li W, Gao Y, Zhang J, Wang X, Yin F, Li Z, Zhang M (2020) Universal DNA detection realized by peptide based carbon nanotube biosensors. *Nanoscale Adv* 2:717–723 . <https://doi.org/10.1039/C9NA00625G>
  43. Sudibya HG, Ma J, Dong X, Ng S, Li L-J, Liu X-W, Chen P (2009) Interfacing Glycosylated Carbon-Nanotube-Network Devices with Living Cells to Detect Dynamic Secretion of Biomolecules. *Angew Chemie Int Ed* 48:2723–2726 . <https://doi.org/https://doi.org/10.1002/anie.200805514>
  44. Hu FX, Kang YJ, Du F, Zhu L, Xue YH, Chen T, Dai LM, Li CM (2015) Living Cells Directly Growing on a DNA/Mn<sub>3</sub>(PO<sub>4</sub>)<sub>2</sub>-Immobilized and Vertically Aligned CNT Array as a Free-Standing Hybrid Film for Highly Sensitive In Situ Detection of Released Superoxide Anions. *Adv Funct Mater* 25:5924–5932 . <https://doi.org/https://doi.org/10.1002/adfm.201502341>
  45. Jin H, Heller DA, Kalbacova M, Kim J-H, Zhang J, Boghossian AA, Maheshri N, Strano MS (2010) Detection of single-molecule H<sub>2</sub>O<sub>2</sub> signalling from epidermal growth factor receptor using fluorescent single-walled carbon nanotubes. *Nat Nanotechnol* 5:302–309 . <https://doi.org/10.1038/nnano.2010.24>
  46. Iverson NM, Barone PW, Shandell M, Trudel LJ, Sen S, Sen F, Ivanov V, Atolia E, Farias E, McNicholas TP, Reuel N, Parry NMA, Wogan GN, Strano MS (2013) In vivo biosensing via tissue-localizable near-infrared-fluorescent single-walled carbon nanotubes. *Nat Nanotechnol* 8:873–880 . <https://doi.org/10.1038/nnano.2013.222>
  47. Hong H, Gao T, Cai W (2009) Molecular Imaging with Single-Walled Carbon Nanotubes. *Nano Today* 4:252–261 . <https://doi.org/10.1016/j.nantod.2009.04.002>
  48. Welsher K, Liu Z, Sherlock SP, Robinson JT, Chen Z, Darancioglu D, Dai H (2009) A route to brightly fluorescent carbon nanotubes for near-infrared imaging in mice. *Nat Nanotechnol* 4:773–780 . <https://doi.org/10.1038/nnano.2009.294>
  49. Welsher K, Sherlock SP, Dai H (2011) Deep-tissue anatomical imaging of mice using carbon nanotube fluorophores in the second near-infrared window. *Proc Natl Acad Sci* 108:8943 LP – 8948 . <https://doi.org/10.1073/pnas.1014501108>
  50. Cherukuri P, Bachilo SM, Litovsky SH, Weisman RB (2004) Near-Infrared Fluorescence Microscopy of Single-Walled Carbon Nanotubes in Phagocytic Cells. *J Am Chem Soc* 126:15638–15639 . <https://doi.org/10.1021/ja0466311>
  51. Leeuw TK, Reith RM, Simonette RA, Harden ME, Cherukuri P, Tsyboulski DA, Beckingham KM, Weisman RB (2007) Single-Walled Carbon Nanotubes in the Intact Organism: Near-IR Imaging and Biocompatibility Studies in Drosophila. *Nano Lett* 7:2650–2654 . <https://doi.org/10.1021/nl0710452>
  52. De La Zerda A, Zavaleta C, Keren S, Vaithilingam S, Bodapati S, Liu Z, Levi J, Smith BR, Ma T-J, Oralkan O, Cheng Z, Chen X, Dai H, Khuri-Yakub BT, Gambhir SS (2008) Carbon nanotubes as photoacoustic molecular imaging agents in living mice. *Nat Nanotechnol* 3:557–562 . <https://doi.org/10.1038/nnano.2008.231>
  53. Zerda A de la, Liu Z, Bodapati S, Teed R, Vaithilingam S, Khuri-Yakub BT, Chen X, Dai H, Gambhir SS (2010) Ultrahigh Sensitivity Carbon Nanotube Agents for Photoacoustic Molecular Imaging in Living Mice. *Nano Lett* 10:2168–2172 . <https://doi.org/10.1021/nl100890d>
  54. Green DE, Longtin JP, Sitharaman B (2009) The Effect of Nanoparticle-Enhanced Photoacoustic Stimulation on Multipotent Marrow Stromal Cells. *ACS Nano* 3:2065–2072 . <https://doi.org/10.1021/nn900434p>
  55. Paratala BS, Sitharaman B (2011) Carbon Nanotubes in Regenerative Medicine. In: *Carbon Nanostructures*. pp 27–39
  56. Heller DA, Baik S, Eurell TE, Strano MS (2005) Single-Walled Carbon Nanotube

- Spectroscopy in Live Cells: Towards Long-Term Labels and Optical Sensors. *Adv Mater* 17:2793–2799 . <https://doi.org/https://doi.org/10.1002/adma.200500477>
57. Liu Z, Davis C, Cai W, He L, Chen X, Dai H (2008) Circulation and long-term fate of functionalized, biocompatible single-walled carbon nanotubes in mice probed by Raman spectroscopy. *Proc Natl Acad Sci* 105:1410 . <https://doi.org/10.1073/pnas.0707654105>
  58. Zavaleta C, de la Zerda A, Liu Z, Keren S, Cheng Z, Schipper M, Chen X, Dai H, Gambhir SS (2008) Noninvasive Raman Spectroscopy in Living Mice for Evaluation of Tumor Targeting with Carbon Nanotubes. *Nano Lett* 8:2800–2805 . <https://doi.org/10.1021/nl801362a>
  59. Servant A, Jacobs I, Bussy C, Fabbro C, da Ros T, Pach E, Ballesteros B, Prato M, Nicolay K, Kostarelos K (2016) Gadolinium-functionalised multi-walled carbon nanotubes as a T1 contrast agent for MRI cell labelling and tracking. *Carbon N Y* 97:126–133 . <https://doi.org/https://doi.org/10.1016/j.carbon.2015.08.051>
  60. Mansfield P (2004) Snapshot Magnetic Resonance Imaging (Nobel Lecture). *Angew Chemie Int Ed* 43:5456–5464 . <https://doi.org/https://doi.org/10.1002/anie.200460078>
  61. Sitharaman B, Kissell KR, Hartman KB, Tran LA, Baikalov A, Rusakova I, Sun Y, Khant HA, Ludtke SJ, Chiu W, Laus S, Tóth É, Helm L, Merbach AE, Wilson LJ (2005) Superparamagnetic gadonanotubes are high-performance MRI contrast agents. *Chem Commun* 3915–3917 . <https://doi.org/10.1039/B504435A>
  62. Hong SY, Tobias G, Al-Jamal KT, Ballesteros B, Ali-Boucetta H, Lozano-Perez S, Nellist PD, Sim RB, Finucane C, Mather SJ, Green MLH, Kostarelos K, Davis BG (2010) Filled and glycosylated carbon nanotubes for in vivo radioemitter localization and imaging. *Nat Mater* 9:485–490 . <https://doi.org/10.1038/nmat2766>
  63. Liu Z, Cai W, He L, Nakayama N, Chen K, Sun X, Chen X, Dai H (2007) In vivo biodistribution and highly efficient tumour targeting of carbon nanotubes in mice. *Nat Nanotechnol* 2:47–52 . <https://doi.org/10.1038/nnano.2006.170>
  64. McDevitt MR, Chattopadhyay D, Kappel BJ, Jaggi JS, Schiffman SR, Antczak C, Njardarson JT, Brentjens R, Scheinberg DA (2007) Tumor targeting with antibody-functionalized, radiolabeled carbon nanotubes. *J Nucl Med* 48:1180–1189 . <https://doi.org/10.2967/jnumed.106.039131>
  65. Harrison BS, Atala A (2007) Carbon nanotube applications for tissue engineering. *Biomaterials* 28:344–353 . <https://doi.org/10.1016/j.biomaterials.2006.07.044>
  66. Lovat V, Pantarotto D, Lagostena L, Cacciari B, Grandolfo M, Righi M, Spalluto G, Prato M, Ballerini L (2005) Carbon Nanotube Substrates Boost Neuronal Electrical Signaling. *Nano Lett* 5:1107–1110 . <https://doi.org/10.1021/nl050637m>
  67. Mazzatenta A, Giugliano M, Campidelli S, Gambazzi L, Businaro L, Markram H, Prato M, Ballerini L (2007) Interfacing Neurons with Carbon Nanotubes: Electrical Signal Transfer and Synaptic Stimulation in Cultured Brain Circuits. *J Neurosci* 27:6931 LP – 6936 . <https://doi.org/10.1523/JNEUROSCI.1051-07.2007>
  68. Bédier A, Seichepine F, Flahaut E, Loubinoux I, Vaysse L, Vieu C (2012) Elucidation of the Role of Carbon Nanotube Patterns on the Development of Cultured Neuronal Cells. *Langmuir* 28:17363–17371 . <https://doi.org/10.1021/la304278n>
  69. Matta-Domjan B, King A, Totti S, Matta C, Dover G, Martinez P, Zakhidov A, La Ragione R, Macedo H, Jurewicz I, Dalton A, Velliou EG (2018) Biophysical interactions between pancreatic cancer cells and pristine carbon nanotube substrates: Potential application for pancreatic cancer tissue engineering. *J Biomed Mater Res B Appl Biomater* 106:1637–1644 . <https://doi.org/10.1002/jbm.b.34012>
  70. Correa-Duarte MA, Wagner N, Rojas-Chapana J, Morscizek C, Thie M, Giersig M (2004) Fabrication and Biocompatibility of Carbon Nanotube-Based 3D Networks as Scaffolds for Cell Seeding and Growth. *Nano Lett* 4:2233–2236 . <https://doi.org/10.1021/nl048574f>

71. Jun Han Z, Rider AE, Ishaq M, Kumar S, Kondyurin A, Bilek MMM, Levchenko I, Ostrikov K (Ken) (2013) Carbon nanostructures for hard tissue engineering. *RSC Adv* 3:11058–11072 . <https://doi.org/10.1039/C2RA23306A>
72. Abarrategi A, Gutiérrez MC, Moreno-Vicente C, Hortigüela MJ, Ramos V, López-Lacomba JL, Ferrer ML, del Monte F (2008) Multiwall carbon nanotube scaffolds for tissue engineering purposes. *Biomaterials* 29:94–102 . <https://doi.org/https://doi.org/10.1016/j.biomaterials.2007.09.021>
73. Namgung S, Kim T, Baik KY, Lee M, Nam J-M, Hong S (2011) Fibronectin–Carbon-Nanotube Hybrid Nanostructures for Controlled Cell Growth. *Small* 7:56–61 . <https://doi.org/https://doi.org/10.1002/sml.201001513>
74. Keefer EW, Botterman BR, Romero MI, Rossi AF, Gross GW (2008) Carbon nanotube coating improves neuronal recordings. *Nat Nanotechnol* 3:434–439 . <https://doi.org/10.1038/nnano.2008.174>
75. Baranauskas G, Maggiolini E, Castagnola E, Ansaldo A, Mazzoni A, Angotzi GN, Vato A, Ricci D, Panzeri S, Fadiga L (2011) Carbon nanotube composite coating of neural microelectrodes preferentially improves the multiunit signal-to-noise ratio. *J Neural Eng* 8:66013 . <https://doi.org/10.1088/1741-2560/8/6/066013>
76. Lee HJ, Park J, Yoon OJ, Kim HW, Lee DY, Kim DH, Lee WB, Lee N-E, Bonventre J V, Kim SS (2011) Amine-modified single-walled carbon nanotubes protect neurons from injury in a rat stroke model. *Nat Nanotechnol* 6:121–125 . <https://doi.org/10.1038/nnano.2010.281>
77. Cellot G, Cilia E, Cipollone S, Rancic V, Sucapane A, Giordani S, Gambazzi L, Markram H, Grandolfo M, Scaini D, Gelain F, Casalis L, Prato M, Giugliano M, Ballerini L (2009) Carbon nanotubes might improve neuronal performance by favouring electrical shortcuts. *Nat Nanotechnol* 4:126–133 . <https://doi.org/10.1038/nnano.2008.374>
78. Chen Z, Zhang A, Wang X, Zhu J, Fan Y, Yu H, Yang Z (2017) The Advances of Carbon Nanotubes in Cancer Diagnostics and Therapeutics. *J Nanomater* 2017:1–13 . <https://doi.org/10.1155/2017/3418932>
79. Bianco A, Kostarelos K, Partidos CD, Prato M (2005) Biomedical applications of functionalised carbon nanotubes. *Chem Commun* 571–577 . <https://doi.org/10.1039/b410943k>
80. Hasnain MS, Ahmad SA, Hoda MN, Rishishwar S, Rishishwar P, Nayak AK (2019) Stimuli-responsive carbon nanotubes for targeted drug delivery. In: *Stimuli Responsive Polymeric Nanocarriers for Drug Delivery Applications*. Elsevier, pp 321–344
81. Sheikhpour M, Naghinejad M, Kasaeian A, Lohrasbi A, Shahraeini SS, Zomorodbakhsh S (2020) The Applications of Carbon Nanotubes in the Diagnosis and Treatment of Lung Cancer: A Critical Review. *Int J Nanomedicine Volume* 15:7063–7078 . <https://doi.org/10.2147/IJN.S263238>
82. Jain KK (2008) Drug Delivery Systems - An Overview. *Methods Mol Biol* 437:1–50 . [https://doi.org/10.1007/978-1-59745-210-6\\_1](https://doi.org/10.1007/978-1-59745-210-6_1)
83. Tan JM, Karthivashan G, Arulsevan P, Fakurazi S, Hussein MZ (2014) Characterization and in vitro studies of the anticancer effect of oxidized carbon nanotubes functionalized with betulinic acid. *Drug Des Devel Ther* 8:2333–2343 . <https://doi.org/10.2147/DDDT.S70650>
84. Tian Z, Yin M, Ma H, Zhu L, Shen H, Jia N (2011) Supramolecular assembly and antitumor activity of multiwalled carbon nanotube-camptothecin complexes. *J Nanosci Nanotechnol* 11:953–958 . <https://doi.org/10.1166/jnn.2011.3100>
85. Arlt M, Haase D, Hampel S, Oswald S, Bachmatiuk A, Klingeler R, Schulze R, Ritschel M, Leonhardt A, Fuessel S, Büchner B, Kraemer K, Wirth MP (2010) Delivery of carboplatin by carbon-based nanocontainers mediates increased cancer cell death. *Nanotechnology* 21: . <https://doi.org/10.1088/0957-4484/21/33/335101>
86. Guven A, Rusakova IA, Lewis MT, Wilson LJ (2012) Cisplatin@US-tube carbon

- nanocapsules for enhanced chemotherapeutic delivery. *Biomaterials* 33:1455–1461 .  
<https://doi.org/10.1016/j.biomaterials.2011.10.060>
87. Singh N, Sachdev A, Gopinath P (2017) Polysaccharide Functionalized Single Walled Carbon Nanotubes as Nanocarriers for Delivery of Curcumin in Lung Cancer Cells. *J Nanosci Nanotechnol* 18:1534–1541 . <https://doi.org/10.1166/jnn.2018.14222>
  88. Singh RP, Sharma G, Sonali, Singh S, Kumar M, Pandey BL, Koch B, Muthu MS (2016) Vitamin E TPGS conjugated carbon nanotubes improved efficacy of docetaxel with safety for lung cancer treatment. *Colloids Surfaces B Biointerfaces* 141:429–442 .  
<https://doi.org/10.1016/j.colsurfb.2016.02.011>
  89. Singh RP, Sharma G, Sonali, Singh S, Patne SCU, Pandey BL, Koch B, Muthu MS (2016) Effects of transferrin conjugated multi-walled carbon nanotubes in lung cancer delivery. *Mater Sci Eng C* 67:313–325 . <https://doi.org/10.1016/j.msec.2016.05.013>
  90. Singh RP, Sharma G, Sonali, Singh S, Bharti S, Pandey BL, Koch B, Muthu MS (2017) Chitosan-folate decorated carbon nanotubes for site specific lung cancer delivery. *Mater Sci Eng C* 77:446–458 . <https://doi.org/10.1016/j.msec.2017.03.225>
  91. Datir SR, Das M, Singh RP, Jain S (2012) Hyaluronate tethered, “smart” multiwalled carbon nanotubes for tumor-targeted delivery of doxorubicin. *Bioconjug Chem* 23:2201–2213 . <https://doi.org/10.1021/bc300248t>
  92. Heister E, Neves V, Tîlmaciu C, Lipert K, Beltrán VS, Coley HM, Silva SRP, McFadden J (2009) Triple functionalisation of single-walled carbon nanotubes with doxorubicin, a monoclonal antibody, and a fluorescent marker for targeted cancer therapy. *Carbon N Y* 47:2152–2160 . <https://doi.org/10.1016/j.carbon.2009.03.057>
  93. Gu YJ, Cheng J, Jin J, Cheng SH, Wong WT (2011) Development and evaluation of pH-responsive single-walled carbon nanotube-doxorubicin complexes in cancer cells. *Int J Nanomedicine* 6:2889–2898 . <https://doi.org/10.2147/ijn.s25162>
  94. Zhang X, Meng L, Lu Q, Fei Z, Dyson PJ (2009) Targeted delivery and controlled release of doxorubicin to cancer cells using modified single wall carbon nanotubes. *Biomaterials* 30:6041–6047 . <https://doi.org/10.1016/j.biomaterials.2009.07.025>
  95. Wen S, Liu H, Cai H, Shen M, Shi X (2013) Targeted and pH-responsive delivery of doxorubicin to cancer cells using multifunctional dendrimer-modified multi-walled carbon nanotubes. *Adv Healthc Mater* 2:1267–1276 .  
<https://doi.org/10.1002/adhm.201200389>
  96. Ali-Boucetta H, Al-Jamal KT, McCarthy D, Prato M, Bianco A, Kostarelos K (2002) Multiwalled carbon nanotube-doxorubicin supramolecular complexes for cancer therapeutics. *Chem Commun* 8:459–461 . <https://doi.org/10.1039/b712350g>
  97. Lu YJ, Wei KC, Ma CCM, Yang SY, Chen JP (2012) Dual targeted delivery of doxorubicin to cancer cells using folate-conjugated magnetic multi-walled carbon nanotubes. *Colloids Surfaces B Biointerfaces* 89:1–9 .  
<https://doi.org/10.1016/j.colsurfb.2011.08.001>
  98. Niu L, Meng L, Lu Q (2013) Folate-conjugated PEG on single walled carbon nanotubes for targeting delivery of doxorubicin to cancer cells. *Macromol Biosci* 13:735–744 .  
<https://doi.org/10.1002/mabi.201200475>
  99. Al Faraj A, Shaik AS, Halwani R, Alfuraih A (2016) Magnetic Targeting and Delivery of Drug-Loaded SWCNTs Theranostic Nanoprobes to Lung Metastasis in Breast Cancer Animal Model: Noninvasive Monitoring Using Magnetic Resonance Imaging. *Mol Imaging Biol* 18:315–324 . <https://doi.org/10.1007/s11307-015-0902-0>
  100. Lodhi N, Mehra NK, Jain NK (2013) Development and characterization of dexamethasone mesylate anchored on multi walled carbon nanotubes. *J Drug Target* 21:67–76 . <https://doi.org/10.3109/1061186X.2012.729213>
  101. Cao Y, Huang H-Y, Chen L-Q, Du H-H, Cui J-H, Zhang LW, Lee B-J, Cao Q-R (2019) Enhanced Lysosomal Escape of pH-Responsive Polyethylenimine–Betaine Functionalized Carbon Nanotube for the Codelivery of Survivin Small Interfering RNA

- and Doxorubicin. *ACS Appl Mater Interfaces* 11:9763–9776 .  
<https://doi.org/10.1021/acsami.8b20810>
102. Heger Z, Polanska H, Krizkova S, Balvan J, Raudenska M, Dostalova S, Moulick A, Masarik M, Adam V (2017) Co-delivery of VP-16 and Bcl-2-targeted antisense on PEG-grafted oMWCNTs for synergistic in vitro anti-cancer effects in non-small and small cell lung cancer. *Colloids Surfaces B Biointerfaces* 150:131–140 .  
<https://doi.org/10.1016/j.colsurfb.2016.11.023>
  103. Razzazan A, Atyabi F, Kazemi B, Dinarvand R (2016) In vivo drug delivery of gemcitabine with PEGylated single-walled carbon nanotubes. *Mater Sci Eng C* 62:614–625 .  
<https://doi.org/10.1016/j.msec.2016.01.076>
  104. Das M, Datir SR, Singh RP, Jain S (2013) Augmented anticancer activity of a targeted, intracellularly activatable, theranostic nanomedicine based on fluorescent and radiolabeled, methotrexate-folic acid-multiwalled carbon nanotube conjugate. *Mol Pharm* 10:2543–2557 . <https://doi.org/10.1021/mp300701e>
  105. Cirillo G, Vittorio O, Kunhardt D, Valli E, Voli F, Farfalla A, Curcio M, Spizzirri UG, Hampel S (2019) Combining Carbon Nanotubes and Chitosan for the Vectorization of Methotrexate to Lung Cancer Cells. *Materials (Basel)* 12:2889 .  
<https://doi.org/10.3390/ma12182889>
  106. Arya N, Arora A, Vasu KS, Sood AK, Katti DS (2013) Combination of single walled carbon nanotubes/graphene oxide with paclitaxel: A reactive oxygen species mediated synergism for treatment of lung cancer. *Nanoscale* 5:2818–2829 .  
<https://doi.org/10.1039/c3nr33190c>
  107. Sobhani Z, Dinarvand R, Atyabi F, Ghahremani M, Adeli M (2011) Increased paclitaxel cytotoxicity against cancer cell lines using a novel functionalized carbon nanotube. *Int J Nanomedicine* 705 . <https://doi.org/10.2147/IJN.S17336>
  108. Lay CL, Liu HQ, Tan HR, Liu Y (2010) Delivery of paclitaxel by physically loading onto poly(ethylene glycol) (PEG)-graftcarbon nanotubes for potent cancer therapeutics. *Nanotechnology* 21: . <https://doi.org/10.1088/0957-4484/21/6/065101>
  109. Zhang W, Zhang D, Tan J, Cong H (2012) Carbon nanotube exposure sensitize human ovarian cancer cells to paclitaxel. *J Nanosci Nanotechnol* 12:7211–7214 .  
<https://doi.org/10.1166/jnn.2012.6506>
  110. Yu B, Tan L, Zheng R, Tan H, Zheng L (2016) Targeted delivery and controlled release of Paclitaxel for the treatment of lung cancer using single-walled carbon nanotubes. *Mater Sci Eng C* 68:579–584 . <https://doi.org/10.1016/j.msec.2016.06.025>
  111. Feazell RP, Nakayama-Ratchford N, Dai H, Lippard SJ (2007) Soluble single-walled carbon nanotubes as longboat delivery systems for platinum(IV) anticancer drug design. *J Am Chem Soc* 129:8438–8439 . <https://doi.org/10.1021/ja073231f>
  112. Li J, Pant A, Chin CF, Ang WH, Ménard-Moyon C, Nayak TR, Gibson D, Ramaprabhu S, Panczyk T, Bianco A, Pastorin G (2014) In vivo biodistribution of platinum-based drugs encapsulated into multi-walled carbon nanotubes. *Nanomedicine Nanotechnology, Biol Med* 10:1465–1475 . <https://doi.org/10.1016/j.nano.2014.01.004>
  113. Su Y, Hu Y, Wang Y, Xu X, Yuan Y, Li Y, Wang Z, Chen K, Zhang F, Ding X, Li M, Zhou J, Liu Y, Wang W (2017) A precision-guided MWNT mediated reawakening the sunk synergy in RAS for anti-angiogenesis lung cancer therapy. *Biomaterials* 139:75–90 .  
<https://doi.org/10.1016/j.biomaterials.2017.05.046>
  114. Komane PP, Kumar P, Marimuthu T, du Toit LC, Kondiah PPD, Choonara YE, Pillay V (2018) Dexamethasone-loaded, pegylated, vertically aligned, multiwalled carbon nanotubes for potential ischemic stroke intervention. *Molecules* 23: .  
<https://doi.org/10.3390/molecules23061406>
  115. Jia N, Lian Q, Shen H, Wang C, Li X, Yang Z (2007) Intracellular Delivery of Quantum Dots Tagged Antisense Oligodeoxynucleotides by Functionalized Multiwalled Carbon Nanotubes. *Nano Lett* 7:2976–2980 . <https://doi.org/10.1021/nl071114c>

116. Van Den Bossche J, Al-Jamal WT, Tian B, Nunes A, Fabbro C, Bianco A, Prato M, Kostarelos K (2010) Efficient receptor-independent intracellular translocation of aptamers mediated by conjugation to carbon nanotubes. *Chem Commun* 46:7379–7381 . <https://doi.org/10.1039/c0cc02092c>
117. Pan B, Cui D, Xu P, Ozkan C, Feng G, Ozkan M, Huang T, Chu B, Li Q, He R, Hu G (2009) Synthesis and characterization of polyamidoamine dendrimer-coated multi-walled carbon nanotubes and their application in gene delivery systems. *Nanotechnology* 20: . <https://doi.org/10.1088/0957-4484/20/12/125101>
118. Guo C, Al-Jamal WT, Toma FM, Bianco A, Prato M, Al-Jamal KT, Kostarelos K (2015) Design of Cationic Multiwalled Carbon Nanotubes as Efficient siRNA Vectors for Lung Cancer Xenograft Eradication. *Bioconj Chem* 26:1370–1379 . <https://doi.org/10.1021/acs.bioconjchem.5b00249>
119. Singh R, Pantarotto D, McCarthy D, Chaloin O, Hoebeke J, Partidos CD, Briand JP, Prato M, Bianco A, Kostarelos K (2005) Binding and condensation of plasmid DNA onto functionalized carbon nanotubes: Toward the construction of nanotube-based gene delivery vectors. *J Am Chem Soc* 127:4388–4396 . <https://doi.org/10.1021/ja0441561>
120. Mohammadi M, Salmasi Z, Hashemi M, Mosaffa F, Abnous K, Ramezani M (2015) Single-walled carbon nanotubes functionalized with aptamer and piperazine-polyethylenimine derivative for targeted siRNA delivery into breast cancer cells. *Int J Pharm* 485:50–60 . <https://doi.org/10.1016/j.ijpharm.2015.02.031>
121. Varkouhi AK, Foillard S, Lammers T, Schiffelers RM, Doris E, Hennink WE, Storm G (2011) siRNA delivery with functionalized carbon nanotubes. *Int J Pharm* 416:419–425 . <https://doi.org/10.1016/j.ijpharm.2011.02.009>
122. Podesta JE, Al-Jamal KT, Herrero MA, Tian B, Ali-Boucetta H, Hegde V, Bianco A, Prato M, Kostarelos K (2009) Antitumor activity and prolonged survival by carbon-nanotube-mediated therapeutic siRNA silencing in a human lung xenograft model. *Small* 5:1176–1185 . <https://doi.org/10.1002/smll.200801572>
123. Al-Jamal KT, Gherardini L, Bardi G, Nunes A, Guo C, Bussy C, Herrero MA, Bianco A, Prato M, Kostarelos K, Pizzorusso T (2011) Functional motor recovery from brain ischemic insult by carbon nanotube-mediated siRNA silencing. *Proc Natl Acad Sci U S A* 108:10952–10957 . <https://doi.org/10.1073/pnas.1100930108>
124. Ladeira MS, Andrade VA, Gomes ERM, Aguiar CJ, Moraes ER, Soares JS, Silva EE, Lacerda RG, Ladeira LO, Jorio A, Lima P, Fatima Leite M, Resende RR, Guatimosim S (2010) Highly efficient siRNA delivery system into human and murine cells using single-wall carbon nanotubes. *Nanotechnology* 21: . <https://doi.org/10.1088/0957-4484/21/38/385101>
125. Kam NWS, Liu Z, Dai H (2005) Functionalization of carbon nanotubes via cleavable disulfide bonds for efficient intracellular delivery of siRNA and potent gene silencing. *J Am Chem Soc* 127:12492–12493 . <https://doi.org/10.1021/ja053962k>
126. Chen H, Ma X, Li Z, Shi Q, Zheng W, Liu Y, Wang P (2012) Functionalization of single-walled carbon nanotubes enables efficient intracellular delivery of siRNA targeting MDM2 to inhibit breast cancer cells growth. *Biomed Pharmacother* 66:334–338 . <https://doi.org/10.1016/j.biopha.2011.12.005>
127. Bartholomeusz G, Cherukuri P, Kingston J, Cognet L, Lemos R, Leeuw TK, Gumbiner-Russo L, Weisman RB, Powis G (2009) In vivo therapeutic silencing of hypoxia-inducible factor 1 alpha (HIF-1 $\alpha$ ) using single-walled carbon nanotubes noncovalently coated with siRNA. *Nano Res* 2:279–291 . <https://doi.org/10.1007/s12274-009-9026-7>
128. Sanz V, Coley HM, Silva SRP, McFadden J (2012) Modeling the binding of peptides on carbon nanotubes and their use as protein and DNA carriers. *J Nanoparticle Res* 14: . <https://doi.org/10.1007/s11051-011-0695-2>
129. Kam NWS, Jessop TC, Wender PA, Dai H (2004) Nanotube molecular transporters: Internalization of carbon nanotube-protein conjugates into mammalian cells. *J Am*



- Chem Soc 126:6850–6851 . <https://doi.org/10.1021/ja0486059>
130. Chen C, Hou L, Zhang H, Zhu L, Zhang H, Zhang C, Shi J, Wang L, Jia X, Zhang Z (2013) Single-walled carbon nanotubes mediated targeted tamoxifen delivery system using asparagine-glycine-arginine peptide. *J Drug Target* 21:809–821 . <https://doi.org/10.3109/1061186X.2013.829071>
  131. Zakaria AB, Picaud F, Rattier T, Pudlo M, Saviot L, Chassagnon R, Lherminier J, Gharbi T, Micheau O, Herlem G (2015) Nanovectorization of TRAIL with single wall carbon nanotubes enhances tumor cell killing. *Nano Lett* 15:891–895 . <https://doi.org/10.1021/nl503565t>
  132. Parra J, Abad-Somovilla A, Mercader J V., Taton TA, Abad-Fuentes A (2013) Carbon nanotube-protein carriers enhance size-dependent self-adjuvant antibody response to haptens. *J Control Release* 170:242–251 . <https://doi.org/10.1016/j.jconrel.2013.05.019>
  133. Li C, Yang K, Zhang Y, Tang H, Yan F, Tan L, Xie Q, Yao S (2011) Highly biocompatible multi-walled carbon nanotube-chitosan nanoparticle hybrids as protein carriers. *Acta Biomater* 7:3070–3077 . <https://doi.org/10.1016/j.actbio.2011.05.005>
  134. Weng X, Wang M, Ge J, Yu S, Liu B, Zhong J, Kong J (2009) Carbon nanotubes as a protein toxin transporter for selective HER2-positive breast cancer cell destruction. *Mol Biosyst* 5:1224–1231 . <https://doi.org/10.1039/b906948h>
  135. Zhu Z, Tang Z, Phillips JA, Yang R, Wang H, Tan W (2008) Regulation of singlet oxygen generation using single-walled carbon nanotubes. *J Am Chem Soc* 130:10856–10857 . <https://doi.org/10.1021/ja802913f>
  136. Marangon I, Ménard-Moyon C, Silva AKA, Bianco A, Luciani N, Gazeau F (2016) Synergic mechanisms of photothermal and photodynamic therapies mediated by photosensitizer/carbon nanotube complexes. *Carbon N Y* 97:110–123 . <https://doi.org/10.1016/j.carbon.2015.08.023>
  137. Gobin AM, Lee MH, Halas NJ, James WD, Drezek RA, West JL (2007) Near-infrared resonant nanoshells for combined optical imaging and photothermal cancer therapy. *Nano Lett* 7:1929–1934 . <https://doi.org/10.1021/nl070610y>
  138. Nomura S, Morimoto Y, Tsujimoto H, Arake M, Harada M, Saitoh D, Hara I, Ozeki E, Satoh A, Takayama E, Hase K, Kishi Y, Ueno H (2020) Highly reliable, targeted photothermal cancer therapy combined with thermal dosimetry using a near-infrared absorbent. *Sci Rep* 10:1–7 . <https://doi.org/10.1038/s41598-020-66646-x>
  139. Brennan ME, Coleman JN, Drury A, Lahr B, Kobayashi T, Blau WJ (2003) Nonlinear photoluminescence from van Hove singularities in multiwalled carbon nanotubes. *Opt Lett* 28:266 . <https://doi.org/10.1364/ol.28.000266>
  140. Gannon CJ, Cherukuri P, Yakobson BI, Cognet L, Kanzius JS, Kittrell C, Weisman RB, Pasquali M, Schmidt HK, Smalley RE, Curley SA (2007) Carbon nanotube-enhanced thermal destruction of cancer cells in a noninvasive radiofrequency field. *Cancer* 110:2654–2665 . <https://doi.org/10.1002/cncr.23155>
  141. O’Connell MJ, Bachilo SH, Huffman CB, Moore VC, Strano MS, Haroz EH, Rialon KL, Boul PJ, Noon WH, Kittrell C, Ma J, Hauge RH, Weisman RB, Smalley RE (2002) Band gap fluorescence from individual single-walled carbon nanotubes. *Science (80- )* 297:593–596 . <https://doi.org/10.1126/science.1072631>
  142. Ghosh S, Dutta S, Gomes E, Carroll D, D’Agostino R, Olson J, Guthold M, Gmeiner WH (2009) Increased heating efficiency and selective thermal ablation of malignant tissue with DNA-encased multiwalled carbon nanotubes. *ACS Nano* 3:2667–2673 . <https://doi.org/10.1021/nn900368b>
  143. Shao N, Lu S, Wickstrom E, Panchapakesan B (2007) Integrated molecular targeting of IGF1R and HER2 surface receptors and destruction of breast cancer cells using single wall carbon nanotubes. *Nanotechnology* 18: . <https://doi.org/10.1088/0957-4484/18/31/315101>
  144. Zhou F, Xing D, Ou Z, Wu B, Resasco DE, Chen WR (2009) Cancer photothermal therapy

- in the near-infrared region by using single-walled carbon nanotubes. *J Biomed Opt* 14:021009 . <https://doi.org/10.1117/1.3078803>
145. Xiao Y, Gao X, Taratula O, Treado S, Urbas A, Holbrook RD, Cavicchi RE, Avedisian CT, Mitra S, Savla R, Wagner PD, Srivastava S, He H (2009) Anti-HER2 IgY antibody-functionalized single-walled carbon nanotubes for detection and selective destruction of breast cancer cells. *BMC Cancer* 9:351 . <https://doi.org/10.1186/1471-2407-9-351>
  146. Moon HK, Lee SH, Choi HC (2009) In vivo near-infrared mediated tumor destruction by photothermal effect of carbon nanotubes. *ACS Nano* 3:3707–3713 . <https://doi.org/10.1021/nn900904h>
  147. Huang N, Wang H, Zhao J, Lui H, Korbelik M, Zeng H (2010) Single-wall carbon nanotubes assisted photothermal cancer therapy: Animal study with a murine model of squamous cell carcinoma. *Lasers Surg Med* 42:798–808 . <https://doi.org/10.1002/lsm.20968>
  148. Zhou F, Wu S, Wu B, Chen WR, Xing D (2011) Mitochondria-targeting single-walled carbon nanotubes for cancer photothermal therapy. *Small* 7:2727–2735 . <https://doi.org/10.1002/smll.201100669>
  149. Zhou F, Wu S, Song S, Chen WR, Resasco DE, Xing D (2012) Antitumor immunologically modified carbon nanotubes for photothermal therapy. *Biomaterials* 33:3235–3242 . <https://doi.org/10.1016/j.biomaterials.2011.12.029>
  150. Wang L, Shi J, Zhang H, Li H, Gao Y, Wang Z, Wang H, Li L, Zhang C, Chen C, Zhang Z, Zhang Y (2013) Synergistic anticancer effect of RNAi and photothermal therapy mediated by functionalized single-walled carbon nanotubes. *Biomaterials* 34:262–274 . <https://doi.org/10.1016/j.biomaterials.2012.09.037>
  151. Oh Y, Jin JO, Oh J (2017) Photothermal-triggered control of sub-cellular drug accumulation using doxorubicin-loaded single-walled carbon nanotubes for the effective killing of human breast cancer cells. *Nanotechnology* 28: . <https://doi.org/10.1088/1361-6528/aa5d7d>
  152. Torti S V., Byrne F, Whelan O, Levi N, Ucer B, Schmid M, Torti FM, Akman S, Liu J, Ajayan PM, Nalamasu O, Carroll DL (2007) Thermal ablation therapeutics based on CNx multi-walled nanotubes. *Int J Nanomedicine* 2:707–714
  153. Wang CH, Huang YJ, Chang CW, Hsu WM, Peng CA (2009) In vitro photothermal destruction of neuroblastoma cells using carbon nanotubes conjugated with GD2 monoclonal antibody. *Nanotechnology* 20: . <https://doi.org/10.1088/0957-4484/20/31/315101>
  154. Burke A, Ding X, Singh R, Kraft RA, Levi-Polyachenko N, Rylander MN, Szot C, Buchanan C, Whitney J, Fisher J, Hatcher HC, D'Agostino R, Kock ND, Ajayan PM, Carroll DL, Akman S, Torti FM, Torti S V. (2009) Long-term survival following a single treatment of kidney tumors with multiwalled carbon nanotubes and near-infrared radiation. *Proc Natl Acad Sci U S A* 106:12897–12902 . <https://doi.org/10.1073/pnas.0905195106>
  155. Burlaka A, Lukin S, Prylutska S, Remeniak O, Prylutsky Y, Shuba M, Maksimenko S, Ritter U, Scharff P (2010) Hyperthermic effect of multi-walled carbon nanotubes stimulated with near infrared irradiation for anticancer therapy: In vitro studies. *Exp Oncol* 32:48–50
  156. Suo X, Eldridge BN, Zhang H, Mao C, Min Y, Sun Y, Singh R, Ming X (2018) P-Glycoprotein-targeted photothermal therapy of drug-resistant cancer cells using antibody-conjugated carbon nanotubes. *ACS Appl Mater Interfaces* 10:33464–33473 . <https://doi.org/10.1021/acsami.8b11974>
  157. Triesscheijn M, Baas P, Schellens JHM, Stewart FA (2006) Photodynamic therapy in oncology. *Oncologist* 11:1034–1044 . <https://doi.org/10.1634/theoncologist.11-9-1034>
  158. Zhu S, Gu Z (2018) Lanthanide-doped materials as dual imaging and therapeutic agents. Elsevier Inc.
  159. Erbas S, Gorgulu A, Kocakusakogullari M, Akkaya EU (2009) Non-covalent functionalized

- SWNTs as delivery agents for novel Bodipy-based potential PDT sensitizers. *Chem Commun* 4956–4958 . <https://doi.org/10.1039/b908485a>
160. Xiao H, Zhu B, Wang D, Pang Y, He L, Ma X, Wang R, Jin C, Chen Y, Zhu X (2012) Photodynamic effects of chlorin e6 attached to single wall carbon nanotubes through noncovalent interactions. *Carbon N Y* 50:1681–1689 . <https://doi.org/10.1016/j.carbon.2011.12.013>
  161. Wang L, Shi J, Liu R, Liu Y, Zhang J, Yu X, Gao J, Zhang C, Zhang Z (2014) Photodynamic effect of functionalized single-walled carbon nanotubes: a potential sensitizer for photodynamic therapy. *Nanoscale* 6:4642–4651 . <https://doi.org/10.1039/c3nr06835h>
  162. Zhang P, Huang H, Huang J, Chen H, Wang J, Qiu K, Zhao D, Ji L, Chao H (2015) Noncovalent ruthenium(II) complexes-single-walled carbon nanotube composites for bimodal photothermal and photodynamic therapy with near-infrared irradiation. *ACS Appl Mater Interfaces* 7:23278–23290 . <https://doi.org/10.1021/acsami.5b07510>
  163. Shi J, Ma R, Wang L, Zhang J, Liu R, Li L, Liu Y, Hou L, Yu X, Gao J, Zhang Z (2013) The application of hyaluronic acid-derivatized carbon nanotubes in hematoporphyrin monomethyl ether-based photodynamic therapy for in vivo and in vitro cancer treatment. *Int J Nanomedicine* 8:2361–2373 . <https://doi.org/10.2147/IJN.S45407>
  164. Girardello R, Baranzini N, Tettamanti G, de Eguileor M, Grimaldi A (2017) Cellular responses induced by multi-walled carbon nanotubes: in vivo and in vitro studies on the medicinal leech macrophages. *Sci Rep* 7:8871 . <https://doi.org/10.1038/s41598-017-09011-9>
  165. Madani SY, Mandel A, Seifalian AM (2013) A concise review of carbon nanotube’s toxicology. *Nano Rev* 4:21521 . <https://doi.org/10.3402/nano.v4i0.21521>
  166. Wang JTW, Fabbro C, Venturelli E, Ménard-Moyon C, Chaloin O, Da Ros T, Methven L, Nunes A, Sosabowski JK, Mather SJ, Robinson MK, Amadou J, Prato M, Bianco A, Kostarelos K, Al-Jamal KT (2014) The relationship between the diameter of chemically-functionalized multi-walled carbon nanotubes and their organ biodistribution profiles in vivo. *Biomaterials* 35:9517–9528 . <https://doi.org/10.1016/j.biomaterials.2014.07.054>
  167. Lindberg HK, Falck GC, Suhonen S, Vippola M, Vanhala E, Catalán J, Savolainen K, Norppa H (2009) Genotoxicity of nanomaterials: DNA damage and micronuclei induced by carbon nanotubes and graphite nanofibres in human bronchial epithelial cells in vitro. *Toxicol Lett* 186:166–173 . <https://doi.org/10.1016/j.toxlet.2008.11.019>
  168. Liu Y, Zhao Y, Sun B, Chen C (2013) Understanding the Toxicity of Carbon Nanotubes. *Acc Chem Res* 46:702–713 . <https://doi.org/10.1021/ar300028m>
  169. Kobayashi N, Izumi H, Morimoto Y (2017) Review of toxicity studies of carbon nanotubes. *J Occup Health* 59:394–407 . <https://doi.org/10.1539/joh.17-0089-RA>
  170. Yu S, Su X, Du J, Wang J, Gao Y, Zhang L, Chen L, Yang Y, Liu X (2018) The cytotoxicity of water-soluble carbon nanotubes on human embryonic kidney and liver cancer cells. *New Carbon Mater* 33:36–45 . [https://doi.org/10.1016/S1872-5805\(18\)60325-7](https://doi.org/10.1016/S1872-5805(18)60325-7)
  171. Knudsen KB, Berthing T, Jackson P, Poulsen SS, Mortensen A, Jacobsen NR, Skaug V, Szarek J, Hougaard KS, Wolff H, Wallin H, Vogel U (2019) Physicochemical predictors of Multi-Walled Carbon Nanotube-induced pulmonary histopathology and toxicity one year after pulmonary deposition of 11 different Multi-Walled Carbon Nanotubes in mice. *Basic Clin Pharmacol Toxicol* 124:211–227 . <https://doi.org/10.1111/bcpt.13119>
  172. Johansson HKL, Hansen JS, Elfving B, Lund SP, Kyjovska ZO, Loft S, Barfod KK, Jackson P, Vogel U, Hougaard KS (2017) Airway exposure to multi-walled carbon nanotubes disrupts the female reproductive cycle without affecting pregnancy outcomes in mice. *Part Fibre Toxicol* 14:17 . <https://doi.org/10.1186/s12989-017-0197-1>
  173. Xu C, Liu Q, Liu H, Zhang C, Shao W, Gu A (2016) Toxicological assessment of multi-walled carbon nanotubes in vitro: potential mitochondria effects on male reproductive

- cells. *Oncotarget* 7:39270–39278 . <https://doi.org/10.18632/oncotarget.9689>
174. Facciola A, Visalli G, La Maestra S, Ceccarelli M, D'Aleo F, Nunnari G, Pellicano GF, Di Pietro A (2019) Carbon nanotubes and central nervous system: Environmental risks, toxicological aspects and future perspectives. *Environ Toxicol Pharmacol* 65:23–30 . <https://doi.org/https://doi.org/10.1016/j.etap.2018.11.006>
  175. Czarny B, Georgin D, Berthon F, Plastow G, Pinault M, Patriarche G, Thuleau A, L'Hermite MM, Taran F, Dive V (2014) Carbon Nanotube Translocation to Distant Organs after Pulmonary Exposure: Insights from in Situ <sup>14</sup>C-Radiolabeling and Tissue Radioimaging. *ACS Nano* 8:5715–5724 . <https://doi.org/10.1021/nn500475u>
  176. Ali-Boucetta H, Kostarelos K (2013) Pharmacology of carbon nanotubes: Toxicokinetics, excretion and tissue accumulation. *Adv Drug Deliv Rev* 65:2111–2119 . <https://doi.org/https://doi.org/10.1016/j.addr.2013.10.004>
  177. Jain S, Thakare VS, Das M, Godugu C, Jain AK, Mathur R, Chuttani K, Mishra AK (2011) Toxicity of Multiwalled Carbon Nanotubes with End Defects Critically Depends on Their Functionalization Density. *Chem Res Toxicol* 24:2028–2039 . <https://doi.org/10.1021/tx2003728>
  178. Li Z, Liu T, Long J, Wu Y, Yan B, Ma P, Cao Y (2019) The toxicity of hydroxylated and carboxylated multi-walled carbon nanotubes to human endothelial cells was not exacerbated by ER stress inducer. *Chinese Chem Lett* 30:582–586 . <https://doi.org/https://doi.org/10.1016/j.ccllet.2018.12.011>
  179. Hindumathi R, Jagannatham M, Haridoss P, Sharma CP (2018) Novel nano-cocoon like structures of polyethylene glycol multiwalled carbon nanotubes for biomedical applications. *Nano-Structures and Nano-Objects* 13:30–35
  180. De Marchi L, Oliva M, Freitas R, Neto V, Figueira E, Chiellini F, Morelli A, Soares AMVM, Pretti C (2019) Toxicity evaluation of carboxylated carbon nanotubes to the reef-forming tubeworm *Ficopomatus enigmaticus* (Fauvel, 1923). *Mar Environ Res* 143:1–9 . <https://doi.org/https://doi.org/10.1016/j.marenvres.2018.10.015>
  181. Qu G, Bai Y, Zhang Y, Jia Q, Zhang W, Yan B (2009) The effect of multiwalled carbon nanotube agglomeration on their accumulation in and damage to organs in mice. *Carbon N Y* 47:2060–2069 . <https://doi.org/https://doi.org/10.1016/j.carbon.2009.03.056>
  182. Yang S-T, Wang X, Jia G, Gu Y, Wang T, Nie H, Ge C, Wang H, Liu Y (2008) Long-term accumulation and low toxicity of single-walled carbon nanotubes in intravenously exposed mice. *Toxicol Lett* 181:182–189 . <https://doi.org/https://doi.org/10.1016/j.toxlet.2008.07.020>
  183. Alpatova AL, Shan W, Babica P, Upham BL, Rogensues AR, Masten SJ, Drown E, Mohanty AK, Alocilja EC, Tarabara V V (2010) Single-walled carbon nanotubes dispersed in aqueous media via non-covalent functionalization: Effect of dispersant on the stability, cytotoxicity, and epigenetic toxicity of nanotube suspensions. *Water Res* 44:505–520 . <https://doi.org/https://doi.org/10.1016/j.watres.2009.09.042>
  184. Nam C-W, Kang S-J, Kang YK, Kwak M-K (2011) Cell growth inhibition and apoptosis by SDS-solubilized single-walled carbon nanotubes in normal rat kidney epithelial cells. *Arch Pharm Res* 34:661–669 . <https://doi.org/10.1007/s12272-011-0417-4>
  185. Raffa V, Ciofani G, Nitodas S, Karachalios T, D'Alessandro D, Masini M, Cuschieri A (2008) Can the properties of carbon nanotubes influence their internalization by living cells? *Carbon N Y* 46:1600–1610 . <https://doi.org/https://doi.org/10.1016/j.carbon.2008.06.053>
  186. Murphy FA, Poland CA, Duffin R, Al-Jamal KT, Ali-Boucetta H, Nunes A, Byrne F, Prina-Mello A, Volkov Y, Li S, Mather SJ, Bianco A, Prato M, Macnee W, Wallace WA, Kostarelos K, Donaldson K (2011) Length-dependent retention of carbon nanotubes in the pleural space of mice initiates sustained inflammation and progressive fibrosis on the parietal pleura. *Am J Pathol* 178:2587–2600 .

- <https://doi.org/10.1016/j.ajpath.2011.02.040>
187. Zhao X, Chang S, Long J, Li J, Li X, Cao Y (2019) The toxicity of multi-walled carbon nanotubes (MWCNTs) to human endothelial cells: The influence of diameters of MWCNTs. *Food Chem Toxicol* 126:169–177 .  
<https://doi.org/https://doi.org/10.1016/j.fct.2019.02.026>
  188. Yamashita K, Yoshioka Y, Higashisaka K, Morishita Y, Yoshida T, Fujimura M, Kayamuro H, Nabeshi H, Yamashita T, Nagano K, Abe Y, Kamada H, Kawai Y, Mayumi T, Yoshikawa T, Itoh N, Tsunoda S, Tsutsumi Y (2010) Carbon nanotubes elicit DNA damage and inflammatory response relative to their size and shape. *Inflammation* 33:276–280 .  
<https://doi.org/10.1007/s10753-010-9182-7>
  189. Pulskamp K, Diabaté S, Krug HF (2007) Carbon nanotubes show no sign of acute toxicity but induce intracellular reactive oxygen species in dependence on contaminants. *Toxicol Lett* 168:58–74 . <https://doi.org/https://doi.org/10.1016/j.toxlet.2006.11.001>
  190. Haniu H, Matsuda Y, Takeuchi K, Kim YA, Hayashi T, Endo M (2010) Proteomics-based safety evaluation of multi-walled carbon nanotubes. *Toxicol Appl Pharmacol* 242:256–262 . <https://doi.org/10.1016/j.taap.2009.10.015>
  191. Cheng C, Müller KH, Koziol KKK, Skepper JN, Midgley PA, Welland ME, Porter AE (2009) Toxicity and imaging of multi-walled carbon nanotubes in human macrophage cells. *Biomaterials* 30:4152–4160 .  
<https://doi.org/https://doi.org/10.1016/j.biomaterials.2009.04.019>